Fermilab Library
0 1160 0038885 4

618

MIDWESTERN UNIVERSITIES RESEARCH ASSOCIATION

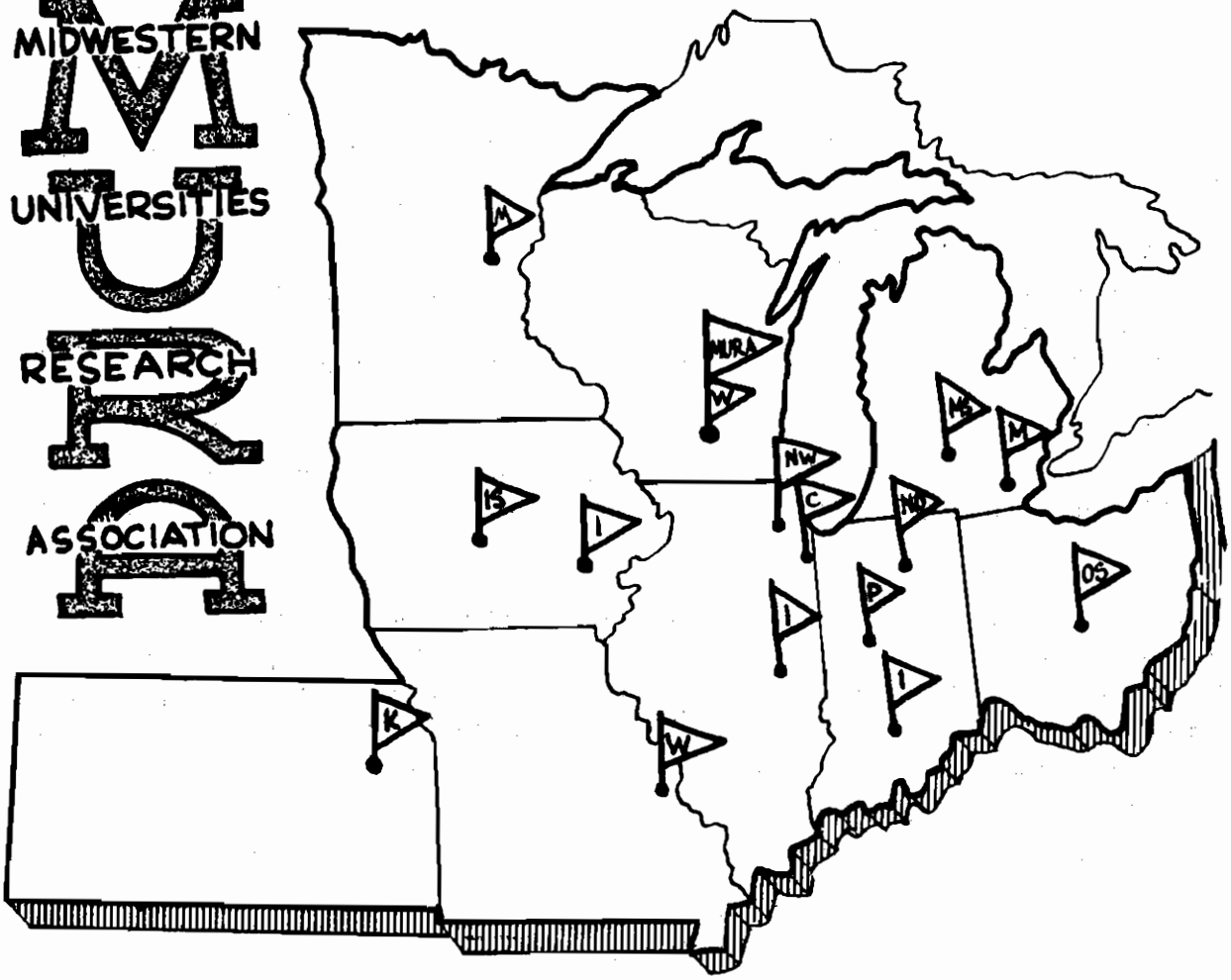

EXPERIMENTAL STRESS ANALYSIS OF A CIRCULAR BUBBLE CHAMBER WINDOW WITH A BEVELED MOUNTING

Andres Peekna and John W. Mark

REPORT **NUMBER** 618

MURA-618
UC-28, Particle Accelerators and
High Voltage Machines
TID-4500 (15th Edition)

MIDWESTERN UNIVERSITIES RESEARCH ASSOCIATION*

2203 University Avenue, Madison, Wisconsin

EXPERIMENTAL STRESS ANALYSIS OF A CIRCULAR BUBBLE CHAMBER WINDOW WITH A BEVELED MOUNTING

Andres Peekna and John W. Mark

May 11, 1961

ABSTRACT

By measuring stresses and deflections of a quarter scale model of a circular bubble chamber window, it was found that mounting the window in a beveled clamp ring decreases the maximum tensile stress in the glass by a factor of two, under the right conditions. The beveled clamp ring exerts an inward force which puts the window under some compression and also exerts a moment which is in a direction opposite to that caused by pressure. The points at which the tensile stress can reach a maximum are the center of the window on the outside, and the edge on the pressure side. The stress at the former point is found to agree well with theory, the stress at the latter point can be predicted with the help of an experimentally determined "stress factor."

It was also found that when an untempered glass plate that is mounted in a beveled clamp ring breaks, it does not leak immediately, the constraint of the beveled clamp ring preventing the cracks from propagating all the way through. Whether this fact has any value for a bubble chamber window is not entirely clear.

* AEC Research and Development Report. Research supported by the U. S. Atomic Energy Commission, Contract No. AT(11-1)-384.

LEGAL NOTICE

This report was prepared as an account of Government sponsored work. Neither the United States, nor the Commission, nor any person acting on behalf of the Commission:

A. Makes any warranty or representation, expressed or implied, with respect to the accuracy, completeness, or usefulness of the information contained in this report, or that the use of any information, apparatus, method, or process disclosed in this report may not infringe privately owned rights; or

B. Assumes any liabilities with respect to the use of, or for damages resulting from the use of any information, apparatus, method, or process disclosed in this report.

As used in the above, "person acting on behalf of the Commission" includes any employee or contractor of the Commission, or employee of such contractor, to the extent that such employee or contractor of the Commission, or employee of such contractor prepares, disseminates, or provides access to, any information pursuant to his employment or contract with the Commission, or his employment with such contractor.

Printed in USA. Price $0.50. Available from the

Office of Technical Services
U. S. Department of Commerce
Washington 25, D. C.

I. DERIVATION OF STRESS FORMULAS

Consider a circular bubble chamber window with a beveled edge. Let us define the symbols: (Figure 1 on next page may clarify some of them more)

R	$\equiv$	Window radius at inside of bevel
R_g	$\equiv$	Gasket central radius
t	$\equiv$	Window thickness
ϕ	$\equiv$	Clamping angle
w	$\equiv$	Width of mounting pad, the inside radius of the lead ring always coinciding with R
μ	$\equiv$	Coefficient of friction on mounting pad
p	$\equiv$	Chamber pressure
F_p	$\equiv$	Pressure perimetral reaction, lbs/inch of perimeter
F_g	$\equiv$	Gasket force, lbs/inch of perimeter
M	$\equiv$	Moment per inch of perimeter due to clamping forces.
S_p	$\equiv$	Stress at center due to chamber pressure alone
S_M	$\equiv$	Stress due to M alone
S_c	$\equiv$	Straight compressive stress due to bevel on clamp ring (alone)
S_{oc}	$\equiv$	Total stress on the outside of the glass at the center
S_{ie}	$\equiv$	Total radial stress on the inside (pressure side) of the glass at the edge
ν	$\equiv$	Poisson's ratio
K	$\equiv$	Experimentally determined "stress factor" used in calculating S_{ie}

Note: In Figure 1 below (and throughout this report) solid arrowheads stand for perimetral reactions, as distinguished from ordinary arrowheads, which indicate dimensions.

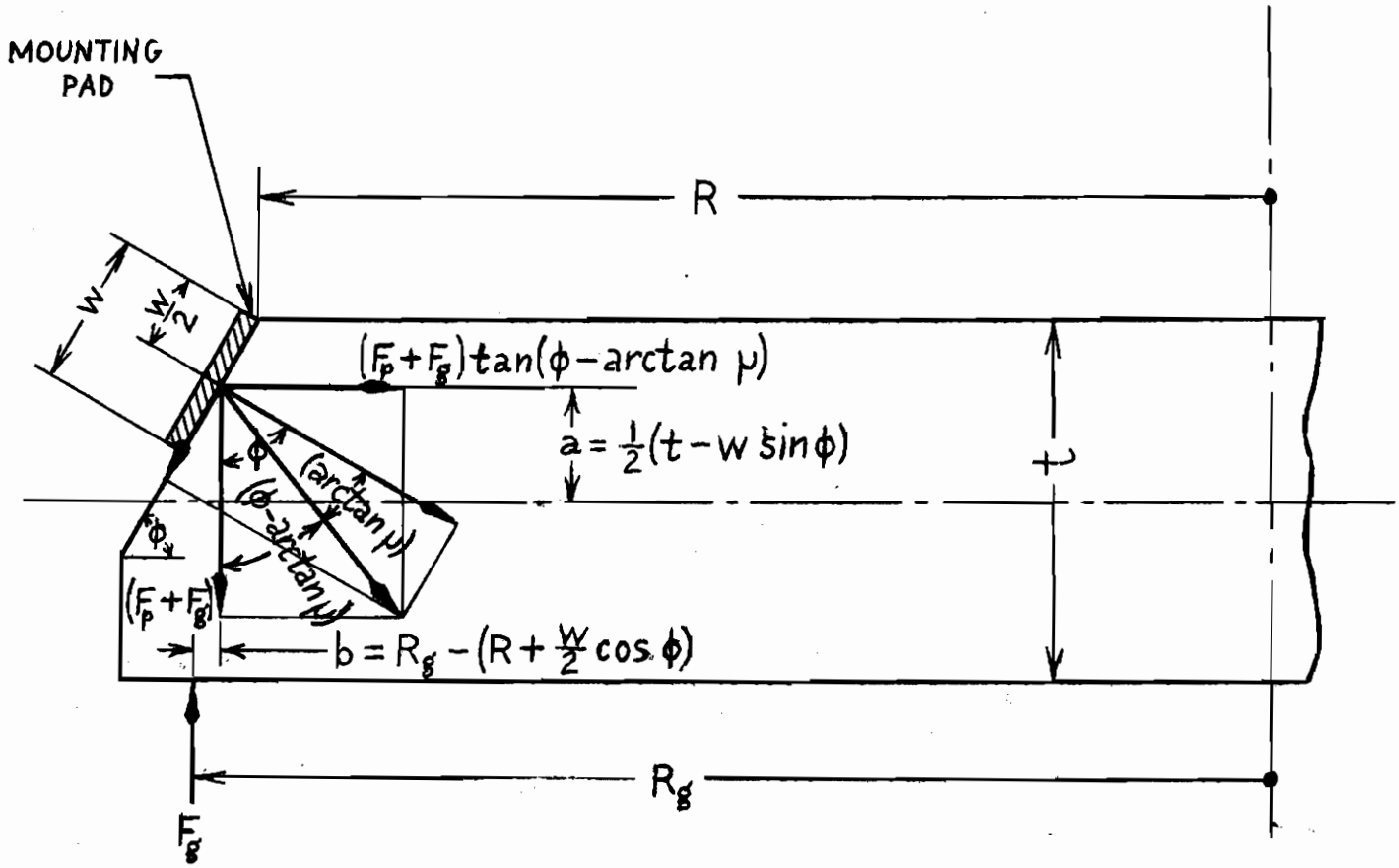

Fig. 1

If we assume that the mounting pad exerts a uniform pressure on the glass then $(F_p + F_g)$ is located at the center of the mounting pad, and it is evident from Figure 1 that

$$M = a(F_p+F_g)\tan(\phi-\arctan\mu) + bF_g$$

where a and b are defined in Figure 1. Further,

$$F_p = \frac{\pi R^2 p}{2\pi R} = \frac{R}{2}p$$

$$M = a\left(\frac{R}{2}p + F_g\right)\tan(\phi - \arctan\mu) + bF_g \tag{1}$$

The stress at center due to pressure alone is given by[1]

$$S_p = \frac{3}{8}(3+\nu)\left(\frac{R}{t}\right)^2 p \tag{2}$$

It is tensile on the outside, compressive on the pressure side.

The stress due to M is given by[2]

$$S_M = \frac{6M}{t^2} \tag{3}$$

It does not vary with the radius and radial stress equals tangential stress throughout the plate in this case. It is compressive on the outside, tensile on the inside.

Finally, it is quite obvious that

$$S_c = \frac{(F_p + F_g)\tan(\phi - \arctan\mu)}{t} \tag{4}$$

and is constant throughout the plate.

Total stress on the outside in the center is obtained easily by superposition:

$$S_{oc} = S_p - (S_M + S_c)$$

Upon substitution:

$$S_{oc} = S_p - \left(\frac{6M}{t^2} + \frac{\left(\frac{R}{2}p + F_g\right)\tan(\phi - \arctan\mu)}{t}\right) \tag{5}$$

where M is, of course, given by (1). Tensile stress has been taken as positive.

---

1 Roark, Formulas for Stress and Strain, 3rd edition. McGraw-Hill, N. Y. 1954. p. 194.

2 Ibid, p. 197.

Now consider the stress on the pressure side at the edge. Let $S_{ie})_a$ = the contribution to S_{ie} due to the horizontal component of the mounting pad reaction (as shown in Figure I, page 3), $S_{ie})_b$ = the contribution to S_{ie} due to F_g not being immediately below the center of the mounting pad, i.e. due to $b \neq 0$. The latter stress can be obtained from (3):

$$S_{ie})_b = \frac{6bF_g}{t^2}$$

$S_{ie})_a$ can be obtained by using (3) and (4):

$$S_{ie})_a = S_M)_a - S_c = \frac{6a(F_p+F_g)\tan(\phi-\arctan\mu)}{t^2} - \frac{(F_p+F_g)\tan(\phi-\arctan\mu)}{t}$$

However, the latter stress would not be expected to be accurately given by the above formula, for (3) assumes a stress distribution like the one in Figure 2, which is a good assumption at the center of the plate, but not good at the edge, for there, because the mounting pad exerts a uniform pressure on the glass, the total stress distribution looks more like the one shown in Figure 3. Hence the stress distribution for S_M cannot be a straight-line one.

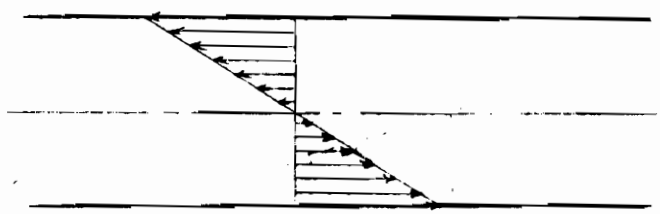

Fig. 2

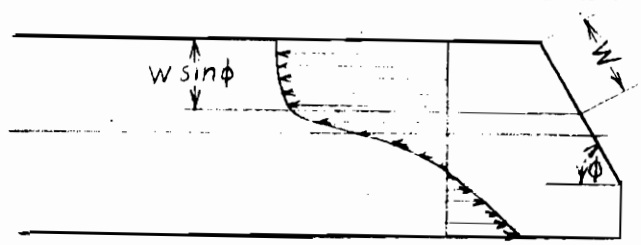

Fig. 3

However, we can still get a useful formula for S_{ie} if we introduce a factor K, to be determined by experiment, such that

$$S_{ie} = K\, S_{ie})_a + S_{ie})_b$$

Then

$$S_{ie} = K\left(\frac{6a}{t^2} - \frac{1}{t}\right)\left(\frac{B}{2}p + F_g\right)\tan(\phi-\arctan\mu) + \frac{6bF_g}{t^2} \qquad (6)$$

The factor K would be expected to change with the value of $\frac{w \sin\phi}{t}$ but for fairly close values of $\frac{w \sin\phi}{t}$, the change should not be too great. The coefficient of friction μ also has to be determined by experiment. It will be seen that we found $\mu \simeq \frac{1}{\sqrt{3}}$ for a lead mounting pad, and K = 2.92 for $\frac{w \sin\phi}{t} = .446$.

Of interest are also the bearing compression on the mounting pad, and the shear on it. Denoting the former by S_b and the latter by τ_b, we have, from Figure I, page 3 :

$$S_b = \frac{1}{w}\left(\frac{R}{2}p + F_g\right)\frac{\cos(\arctan\mu)}{\cos(\phi - \arctan\mu)} \tag{7}$$

$$\tau_b = \mu S_b = \frac{\mu}{w}\left(\frac{R}{2}p + F_g\right)\frac{\cos(\arctan\mu)}{\cos(\phi - \arctan\mu)} \tag{8}$$

II. METHOD OF MEASURING STRESSES EXPERIMENTALLY

The window test fixture assembly is shown in Figure 6, page 21. The window was very nearly a quarter scale model of the MURA 30" H_2 bubble chamber window, and the geometry of the mounting was also similar. The assembly is shown for beveled glass; unbeveled glass was also tested with the same test fixture by turning the clamp ring around.

All stress measurements were done with SR-4 strain gages (Baldwin-Lima-Hamilton Corporation, type AX-7, lot no. B-32 10F608. Resistance: 120 $\pm$ 1 ohms. Gage factor: 1.90 $\pm$ 2%). These gages enabled us to measure strain in two perpendicular directions at the same point. Letting E = modulus of elasticity and ν = Poisson's ratio for the glass, ϵ_x and ϵ_y for strains in two perpendicular directions, we can find the stresses in those directions by[3]

$$S_x = \frac{E}{(1-\nu^2)}(\epsilon_x + \nu\epsilon_y) + \nu(1-\nu)S_z$$

$$S_y = \frac{E}{(1-\nu^2)}(\epsilon_y + \nu\epsilon_x) + \nu(1-\nu)S_z$$

---

3 Timoshenko and Goodier, Theory of Elasticity 2nd ed. N. Y. McGraw-Hill, 1951. Solve equations (3) on page 7 of this book for S_x and S_y.

which is what was done. On the outside of the glass S_z is zero, on the inside it is equal to the negative of the pressure, for tension has been taken as positive. However, The S_z term is so small (it only makes a difference of 40 psi stress at 250 psi pressure) that it was neglected. E was assumed to be equal to 10^7 psi and ν to be equal to .21.[4]

The strain gages were glued on with Dolphon epoxy cement (made by John C. Dolph Company). Dummy compensating gages were glued onto thin pieces of glass which were taped to the test window so that they were located right on top of the measuring gages, to minimize thermal disturbances.

In measuring strain on the pressure side, the dummy gage has pressure exerted on it from all sides, the measuring gage has pressure exerted only on the plane containing . To correct for this effect on the strain gage itself, strain was measured at the center of unbeveled glass both on the outside and the pressure side, the dummy gage for the latter being under pressure, as in all the other measurements of strain on the pressure side. Assuming true strain to be equal and opposite on both sides, the difference in the absolute values of strain readings gives the correction, which was found to be -13 microinches per 50 psi. This was done for two different cases: one with a lead pad between clamp ring and glass, the other with a 3.875" radius teflon O-ring between clamp ring and glass to minimize clamping effects. Both cases gave very nearly the same strain readings, but there was less hysteresis in the readings for the latter case, hence its data were used. When the two compensating gages were hooked up so that the difference in strain between them could

---

4 These values are given for soda-lime plate glass in Shand, Glass Engineering Handbook, 2nd ed., N.Y., McGraw-Hill, 1958. pp. 17 and 37.

be read, it was found to be -15 microinches per 50 psi. But this is not as realistic correction, for in the actual case of measuring strain of the window on the pressure side, there is pressure on the plane containing the strain gage, whereas there was none on the outside dummy gage. So we took -13 microinches per 50 psi as our correction, which means 13 microinches per 50 psi was subtracted from the strain readings on the pressure side. A word of caution here: this value should not be indiscriminately used for other types of strain gages, since it may not be the same for all types.

The fluid for applying the pressure was hydraulic oil. There were two pressure taps in the test fixture, the other serving the purpose of getting the air out. Pressure was measured by an ordinary Bourdon gage, which was calibrated with a dead-weight pressure gage tester.

The gasket force, Fg, was determined by tightening the bolts with a torque wrench which was calibrated by a spring scale. When there is no pressure in the test fixture then

$$\text{Force per bolt} = \frac{2\pi R_g F_g}{\text{no. of bolts}} = \frac{2\pi(3.875)F_g}{16} = 1.522\,F_g$$

in our case, as can be seen from Figure 6, page 21. From UCRL Design Data No. 48, page 1, we get that 1 inch-lb. torque on a 1/2-13-UNC bolt gives 10.9 pounds force on the bolt, thus

$$\text{Torque per bolt} = \frac{\text{Force per bolt}}{10.9} = .1396\,F_g \qquad (9)$$

Since the rubber O-ring is much more elastic than our bolts, we can expect the gasket force to remain very nearly constant as pressure is applied in the test rig.

III. DISCUSSION OF EXPERIMENTALLY OBTAINED STRESSES

For unbeveled glass with a 1/4" wide x 1/16" thick lead pad between glass and clamp ring the stress on the outside at the center was measured. The results are shown on Figures 7, 8 and 9, pages 22-24. It is seen that there is some statistical variation, which was most likely due to the support being not perfectly even all around the edge. At low gasket forces we obtained an average slope of $S_p = 13.4\ p$. At $F_g \simeq 1000$, we obtained a slope of $S = 13.0\ p$, showing that clamping forces do not have much effect on the stress for flat glass of our configuration. We took the average slope to be $S = 13.2\ p$. The formula (2), p.4, on the other hand, gives, for $\nu = 0.21$, $R = 3.75$, $t = .97$,

$$S_p = \frac{3}{8}(3+\nu)\left(\frac{R}{t}\right)^2 p = 18.1\,p$$

showing a 37% difference from the measured value. We have sufficient reason to believe that this difference is not due to clamping forces providing any resisting moment. Deflections, which we could measure more accurately than strains, were very close for the cases when there was a lead pad between glass and clamp ring, and when there was a 3.875" radius teflon O-Ring. (See page 14, in section on deflections)

About a sixth of the difference in S_p can be explained by the fact that there was a 3/8" overhang of the glass plate beyond R. This overhang acts as a stiffening ring, resisting the sloping of the plate edges when the plate deflects. The relation between slope and resisting moment for such a ring is:[5]

$$\theta = \frac{MR^2}{EI}$$

where E is modulus of elasticity of the material and I is the moment of inertia of the cross section of the ring about an axis passing through its centroid and in the plane of the ring. Using the above relation, as well as those giving the slopes

---

[5] Roark, Formulas for Stress and Strain, p. 231.

due to pressure and moment alone, respectively,[6]

$$\theta_p = \frac{3(1-\nu)}{2E}\left(\frac{R}{t}\right)^3 p$$

$$\theta_M = \frac{12(1-\nu)MR}{Et^3}$$

and also relation (2), page 4, it can be obtained by superposition that, letting

c = amount of overhang (3/8" in our case)

$$S\Big)_{\substack{\text{OVERHANG}\\ \text{STIFFENING}}} = -\frac{3\left(\frac{R}{t}\right)^2 p}{4\left(1+\frac{1}{(1-\nu)}\frac{R}{c}\right)} \tag{10}$$

which in our case accounts for about 6% of S_p. It is a rather minor effect in most cases. The minus sign indicates that it decreases S_p. However, the major portion of the difference is probably due to our plate being relatively thick. Roark[7] cautions against expecting accurate results from the flat-plate formulas given in his book for the thickness being more than 1/4 of the least transverse dimension; we do not thus expect perfect agreement in our case, where the thickness is about 1/8 of the diameter. Thus, in calculating stresses for the beveled glass, we will assume the experimental value:

$$S_p = 13.2\,p$$

With beveled glass it was observed that when both mounting pads were lead, the glass would stick in the clamp ring, retaining about 2/3 of the stress and deflection it had before the bolts were loosened, and have to be popped out. When one of them was

---

6 Roark, Formulas for Stress and Strain, p. 194 and p. 196.

7 Ibid, p. 192.

teflon, then the glass would not stick in the clamp ring. The stress behavior, however, was very similar for the two cases. Hence, we assume that the coefficient of pad friction $\mu = \tan 30 \text{ degrees} = \frac{1}{\sqrt{3}}$, since our clamping angle is 60 degrees. For lead pads, it is actually slightly more, for teflon + lead pad, slightly less.

If we put w = 1/2, $\mu = \frac{1}{\sqrt{3}}$, $\phi = 60$ degrees, R = 3.75 into formulas (7) and (8), we get for bearing stresses:

$$S_b = 3.75p + 2F_g$$

$$\tau_b = 2.163p + 1.154F_g$$

These equations are plotted on Figure 10, page 25. Since lead yields at 600 psi compression (hence 300 psi shear) it can be seen from the plot that most of the time we are well beyond the yield point. Hence the assumption that the mounting pad exerts a uniform pressure on the glass is a good one, and thus the theory derived in the previous section can be expected to hold.

From Figure 6, page 21, we can see that $a = \frac{1}{2}(t - w\sin\phi) = .2685$, b = 1/16, t = .97. The value R = 3.75 was used in stress calculations. Using formulas (1) and (5) on page 4, and the experimental value for S_p, we get, for the stress on the outside at the center:

$$S_{oc} = 10.23p - 1.983F_g$$

The dependence of the stress on the pressure side at the edge on F_g was found to agree best if in formula (6), page 5, K is taken to be equal to 2.92. Then we get

$$S_{ie} = 2.15p + 1.550F_g$$

---

[8] Mantell, Engineering Materials Handbook, N. Y.: McGraw-Hill, 1958, p. 8-2.

The above relations are plotted in Figures 11 - 14, pages 26-29, where their agreement with experiment can be seen. At high gasket forces, it is seen that S_{oc} shifts upward with time, S_{ie} downward. This is due to decrease of Fg caused most likely by plastic yielding of mounting pads. It is also seen that the experimental slope of the S_{ie} lines is less than the predicted value; this is due to the center of our strain gage having been located 1/4" inward from the rubber O-ring, where there is a small compressive stress due to pressure. However, this stress cannot be sufficiently well predicted by a formula out of Roark's book, since this point is very near the point of application of the reacting forces. This is why we used only the dependence of S_{ie} on F_g in determining K.

It might seem surprising that S_{oc} for the beveled glass agrees so well with the theory, even though our plate is fairly thick. This is partly due to S_c making up about 40% of (S_m + S_c), which is subtracted from S_p to give S_{oc}. The formula for S_c can be expected to hold exactly for any plate thickness.

IV. DISCUSSION OF DEFLECTIONS

The relative deflections between center and 3.5 inch radius were measured with the following measuring device:

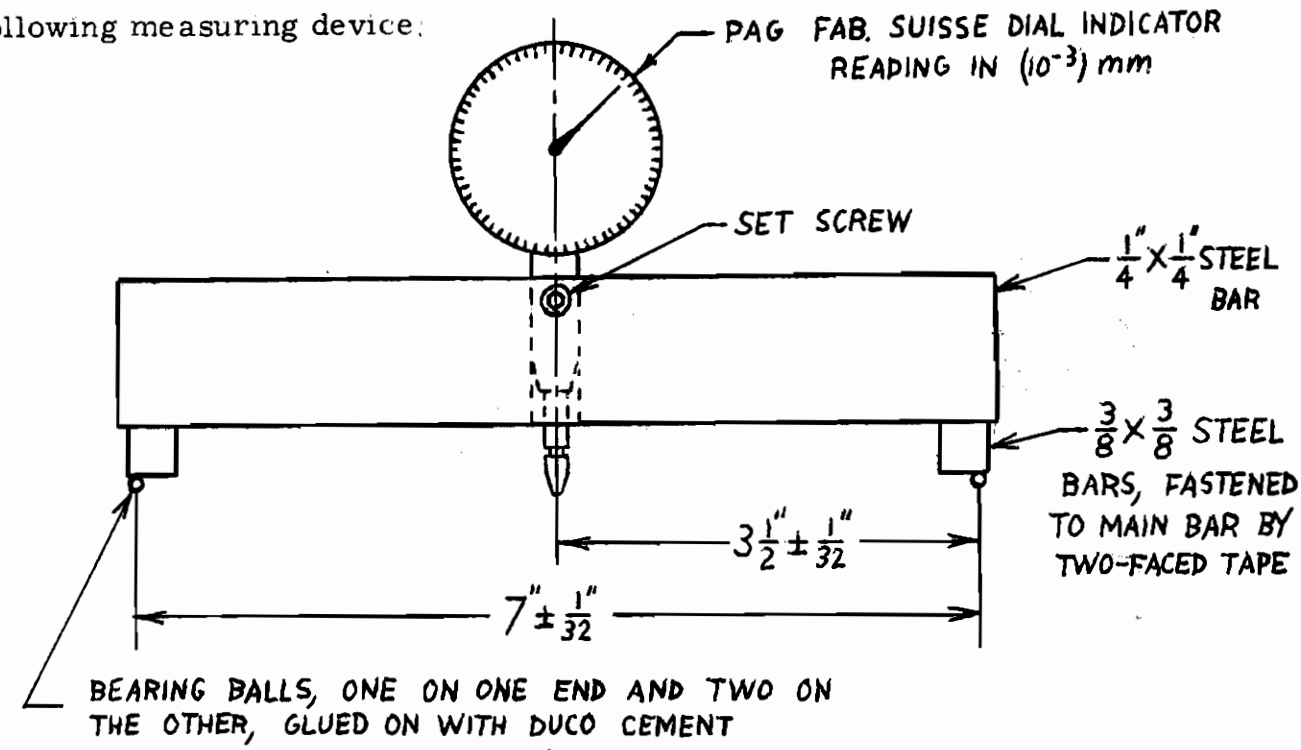

Fig. 4

The relative deflection due to bending of the plate caused by pressure is[9]

$$Y_p = \frac{3}{8}\frac{(1-\nu^2)r^2}{Et^3}\left(\frac{3+\nu}{1+\nu}R^2 - \frac{r^2}{2R^4}\right)p$$

where r is the radius that the deflection of the center is taken relative to, and m and R are defined in the old way, on page 2. In addition, there is also a deflection due to shear and a negative one due to broadening of the inside face of the plate due to pressure because the Poisson's ratio $\nu \neq 0$. They are given by:[10]

$$Y_p\Big)_{SHEAR} = \frac{3r^2}{8Gt}p \quad ; \quad G \equiv \frac{E}{2(1+\nu)}$$

$$Y_p\Big)_{\substack{INSIDE\\BROADENING}} = -\frac{\nu r^2}{2Et}p$$

---

9 Roark, Formulas for Stress and Strain, page 194.

10 Timoshenko, Theory of Plates and Shells, N. Y., McGraw-Hill, pp 79 80.

The last one turns out to be very small. Combining the above, we have:

$$Y_p = \frac{r^2 p}{E t}\left\{\frac{3+\nu}{4} + \frac{3}{8}(1-\nu^2)\left(\frac{R}{t}\right)^2\left(\frac{3+\nu}{1+\nu} - \frac{r^2}{2R^2}\right)\right\} \tag{11}$$

When the glass has a beveled edge, there is also a relative deflection due to edge moment:

$$Y_M = -\frac{6(1-\nu)r^2}{E t^3} M \tag{12}$$

where M is given by relation (1), page 4. The total deflection then becomes:

$$Y = Y_p - \frac{6(1-\nu)r^2}{E t^3} M \tag{13}$$

For an unbeveled piece of glass with lead pad between glass and clamp ring it was found that $Y_p = .370$ p where Y_p is expressed in (10^{-3}) mm and p in psi. The deflection was measured with the measuring device rotated about the center at 45 degree intervals, and the deflections were all so close that no need was seen for presenting them in the form of graphs. It should be noted that these deflections were not for the same case in which the stresses were measured (for the unbeveled glass). Deflections were also measured for unbeveled glass and a 3.875" radius teflon "O"-ring between glass and clamp ring, to minimize clamping effects. In this case, it was found that Yp = .375 p in (10^{-3}) mm, a difference of 1.3%. Hence we are assured that there is no appreciable clamping of the edges of the unbeveled glass in our case, i.e., we have a free-edged plate, and can believe that the stresses and deflections measured for the unbeveled glass are very close to true values of S_p and Y_p.

The formula (11) predicts Yp = .407 p in (10^{-3}) mm for our values of R = 3.75, r = 3.5, t = .97 and assumed ν = .21 and E = 10^7. Half of the difference

is accounted by the stiffening effect of the overhanging edge. In a way similar to the one used for stresses, it can be found that

$$Y)_{\substack{\text{OVERHANG}\\ \text{STIFFENING}}} = -\frac{3(1-\nu)R^2r^2p}{4\left(1-\frac{1}{(1-\nu)}\frac{R}{c}\right)Et^3}$$

which in our case decreases Yp to .389 p. This could be made to agree exactly with the experimental value of .370 p if we assumed E = 10.5 (10^6) instead of the 10 (10^6) which we have assumed. However, there is not sufficient justification to believe the formulas to hold exactly for such a relatively thick plate, hence we stuck with the handbook value of 10^7. At any rate, the difference is not great.

For the beveled glass, putting $a = \frac{1}{2}(t - w\sin\phi) = .2865$, $b = \frac{1}{16}$, $t = .97$, $r = 3.5$, $\nu = .21$ and $E = 10^7$ into formula (13), and using the experimental value $S_p = .370\ p$, we get

$$Y = .3203\ p - .0366\ Fg$$

This equation is plotted on Figures 15-18, pages 30-33, where its extent of agreement with experiment can be seen. It is seen that the deflections seem to tell us a more optimistic story than the stresses as far as the actual value for the coefficient of friction μ is concerned. The reason why the agreement is not as good for the deflections as it is for stresses is probably because for S_M the stress distribution at and near the edge is not a linear one, as mentioned before, whereas in the deflection formula for S_M a straight-line stress distribution is implied throughout the plate. The stress distribution at the edge would not change the stress at the center much, because there what matters is the stress distribution at the center, whereas all portions of the plate influence the deflections. Thus formula (12) is probably not accurate for our case.

In Figure 19, page 34, is a plot of the gasket force vs. deflection at zero pressure for the beveled glass. The symbols ϕ and $+$ indicate deflections measured with the measuring device rotated 90 degrees relative to each other. The

extent of the horizontal and vertical lines crossing the points indicate uncertainties reading the respective quantities, however the actual uncertainty in gasket force is probably larger since it depends on thread friction, which may vary slightly from case to case and also with the load. The plot in Figure 19 shows sufficiently good linearity. between gasket force and deflection of the beveled glass. Hence there is sufficient reason to believe that the stress at zero pressure is also linear in F_g.

V. RESULTS OF BREAKAGE TESTS

We have broken only three plates of glass, one with a beveled edge and width of lead mounting pad $W = \frac{1}{2}''$, another with $W = \frac{3}{8}''$, and one unbeveled plate. Thus we do not have sufficient statistics to base much in the way of conclusions on this, however, the differing behavior at failure is of interest.

The window mounted with $W = \frac{1}{2}''$ had teflon for the other pad (for clarity of configuration see drawing on page 21). The bolts were tightened so that the gasket force was 1,000 lbs./inch. Pressure was applied at 100 psi increments and held for 5 minutes at each value. After 3 minutes at 700 psi the window cracked with a ringing sound. The cracked window did not leak. The window had failed at the center on the outside,as expected, at a predicted stress there of 5,200 psi. The cracks relieved the stresses there, but it seems that the beveled clamp ring prevented the window from deflecting further, hence the cracks did not go all the way through to the pressure side of the glass. The pressure was then slowly raised to 1,000 psi and held there for 2 minutes. Crackling sounds could be heard in the glass as more cracks formed, but the window never leaked. Then pressure as released and after a couple of hours it was applied again. This time it leaked, however. Figure 21 on page 36 shows oil leaking through the cracks of this piece

of glass. Figure 22 shows the other side of the glass after the test fixture was disassembled. The glass held together after being lifted out, as can be seen in Figure 23. But upon further handling it fell apart, as can be seen in Figure 24. It was seen that there were also cracks as shown in the sketch

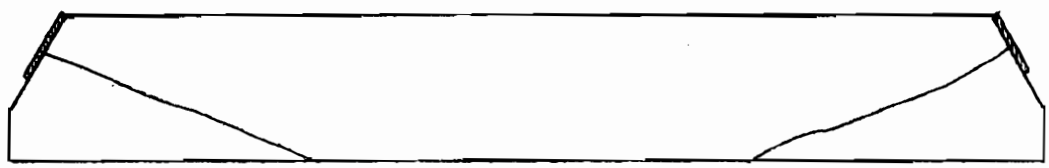

Fig. 5

of the cross section of the window (Fig. 5). They were not seen when the window first cracked at 700 psi. What is more, the radial cracks penetrated through the above ones without any discontinuities, implying that the former formed first. We are not sure really as to whether the cracks in the above sketch occurred between 700 and 1,000 psi or upon releasing the pressure back to zero. They look very much as having resulted from shear stress at the mounting pad. The bearing compression and shear at 1,000 psi can be computed by equations (7) and (8), they become, for our case

$$S_b = 3.75p + 2F_g$$

$$\tau_b = 2.163p + 1.154F_g$$

At p = 1,000, $F_g \doteq 220$ (we use this value because upon checking the bolt torque after the test, F_g had relaxed to this value due to lead mounting pad being compressed to about half its former thickness), we have S_b = 4,200 psi, τ_b = 2,400 psi. Shear stress is same in mutually perpendicular planes, so τ_b contributed to the cause of the crack. There is also some shear due to S_b alone on a plane that is perpendicular to and extends to the middle of the mounting pad,

which is the plane of the cracks that occurred. The sum of these stresses could have caused the cracks. However, it should be emphasized that when the glass was already cracked in the center, there might have been other stresses present. Yet this might indicate that the mounting pad should not be made so narrow that the bearing stresses get very high.

The beveled glass plate with w = 3/8" broke at 300 psi and small gasket force while the bolts were being tightened at that pressure. In all other tests, bolts were tightened only at zero pressure. The stress on the outside at the center as indicated by a strain gage was 3,230 psi. It is possible that the stress was higher in a direction other than the one in which the strain gage was measuring, for while the bolts are being tightened they do not have equal tension, which might cause a wave in the clamp ring. Here again the glass did not leak after cracking. The pressure was immediately reduced to zero and test fixture disassembled. The cracked glass is shown in Figure 25 and Figure 26 on page 37. It can be seen that no crack goes all the way through in this case.

The unbeveled glass plate broke after being held for 3 minutes at 300 psi, at a predicted stress of 4,000 psi. It leaked immediately. Figure 27, page , shows the glass after cracking while still in the test fixture, Figure 28 shows how it fell apart immediately after the test fixture was disassembled.

A conclusion of these breakage tests is that beveled untempered glass in a bubble chamber might possibly prevent an explosion even if it cracks, if the cracking is noticed right away and pressure released. However, there is no guarantee of this, for pulsing may cause it to fall apart. Tempered glass would probably fall apart as soon as it cracked.

VI. PREDICTION OF STRESS BEHAVIOR FOR MURA 30" H_2 BUBBLE CHAMBER WINDOWS

A picture of the 30" H_2 bubble chamber glass and its mounting is shown on Figure 20, page 35. From that picture, we can get that a = 1.412", b = 3/32", (we have assumed the reaction moves up 1/16" because of some rolling of indium wires). R/t is now 15.5/4.125 = 3.76, versus the value of 3.87 for the model. Since S_p depends on $(R/t)^2$, S_p is probably slightly less for the chamber glass than for the model, however we were conservative and assumed it to be the same value of $S_p = 13.2$ p. The factor K in formula (6) is expected to depend on $\frac{w \sin\phi}{t}$, which for the chamber glass is .328, whereas it was .446 for the model, but we will assume that K = 2.92 also for the chamber. Thus we get for the chamber, assuming $\mu = \frac{1}{\sqrt{3}}$ also for indium:

$$S_{oc} = 9.89\,p - .4605\,F_g$$

$$S_{ie} = 3.33\,p + .466\,F_g$$

These relations are plotted on page 35. The chamber will be operated with $F_g = 700$ lbs./inch, which is a value that our inflatable gasket can conveniently maintain. At the operating point of 100 psi pressure, we are on the line of minimum stress, with 665 psi tension in the glass. This is a factor of 2 better than for the unbeveled glass. Our safety valve is set at 150 psi, at that pressure and $F_g = 700$, the maximum tensile stress rises to 1,150 psi, still a factor of 1.7 better than for unbeveled glass. If, however, the inflatable gasket pressure would fail, then the tensile stress at 90 psi goes up to 590 psi, and that at 150 psi goes to 1,480 psi, which is only a factor of 1.335 better than unbeveled glass.

If that occurred, then the pressure would not be maintained for long, for the gasket would leak.

If we assume that the indium wires that act as mounting pads get flattened to the extent that they form a solid mass, then we get for the bearing stresses, using (7) and (8):

$$S_b = 4.77\ p + .615\ F_g$$

$$\tau_b = 2.75\ p + .355\ F_g$$

At 150 psi and Fg = 700, we have then:

$$S_b = 1,145 \text{ psi}$$

$$\tau_b = 660 \text{ psi}$$

The reason indium was used is because lead is too hard at liquid hydrogen temperatures. The reason indium was used in the form of wires rather than as a sheet is to solve two problems: differential shrinkage of about .050" on the diameter between stainless steel clamp ring and the window, and getting the glass out of the clamp ring during disassembly. As it is, the differential shrinkage goes into doing part of the job of flattening the indium wires. Upon warming up, the differential expansion loosens the clamp ring so the glass cannot get stuck in it.

In designing a mounting for a beveled window, the two variables that influence the stresses are the gasket force and mounting pad width, once glass geometry has been fixed. One should pick the highest gasket force one can conveniently apply, and then adjust the mounting pad width so as to be on the line of minimum stress (such as shown in Figure 20, page 35) at the operating pressure. If one picked a lower gasket force then the line of minimum stress would have a higher slope than in the former case.

30" H_2 BUBBLE CHAMBER
$\frac{1}{4}$ SCALE WINDOW TEST FIXTURE ASSEMBLY

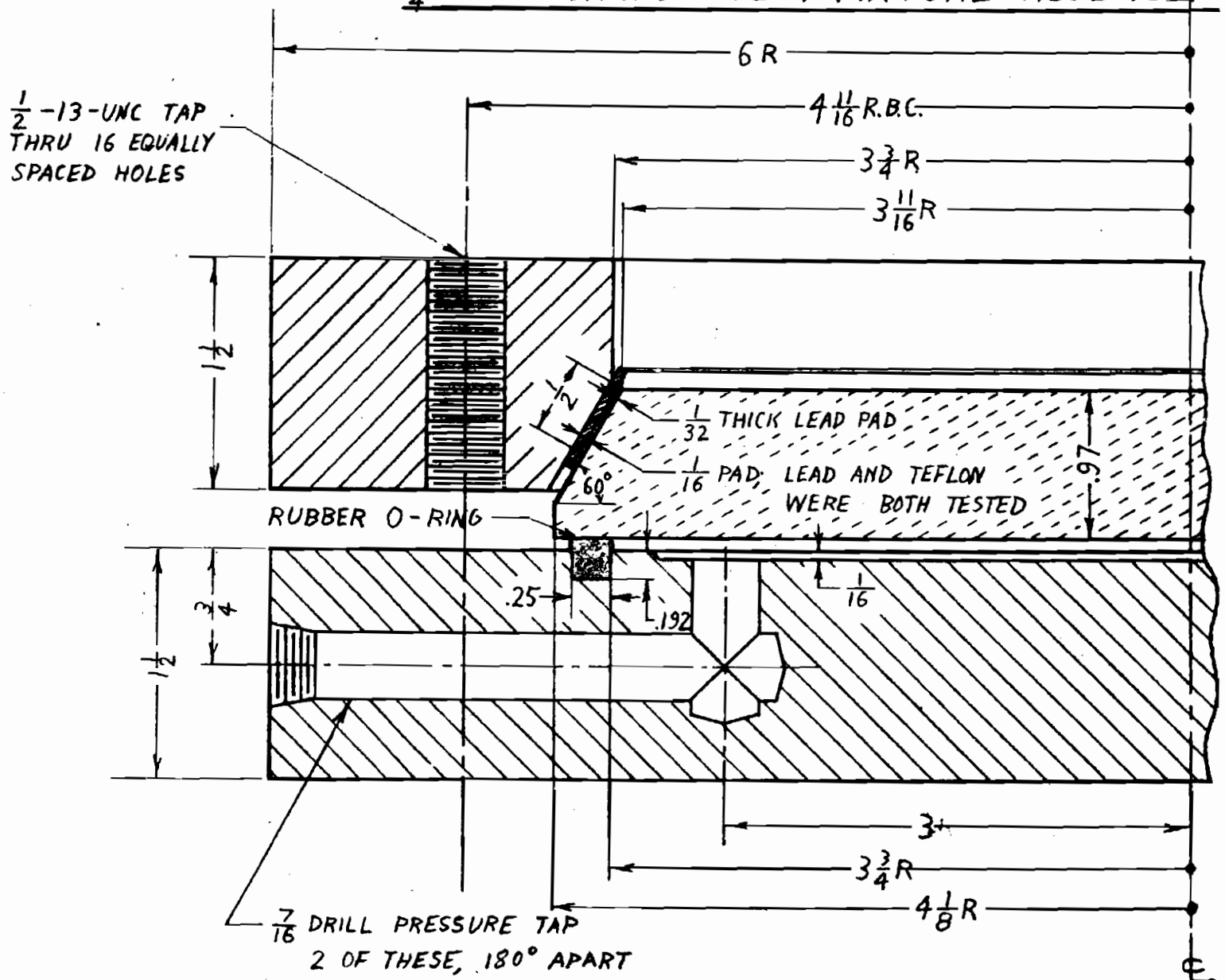

SCALE OF DRAWING: FULL. ALL DIMENSIONS IN INCHES

Midwestern Universities Research Association - Wisconsin
ENGINEERING NOTE
SUBJECT
NAME
DATE
FILE NO.
PAGE 21

FIG. 6

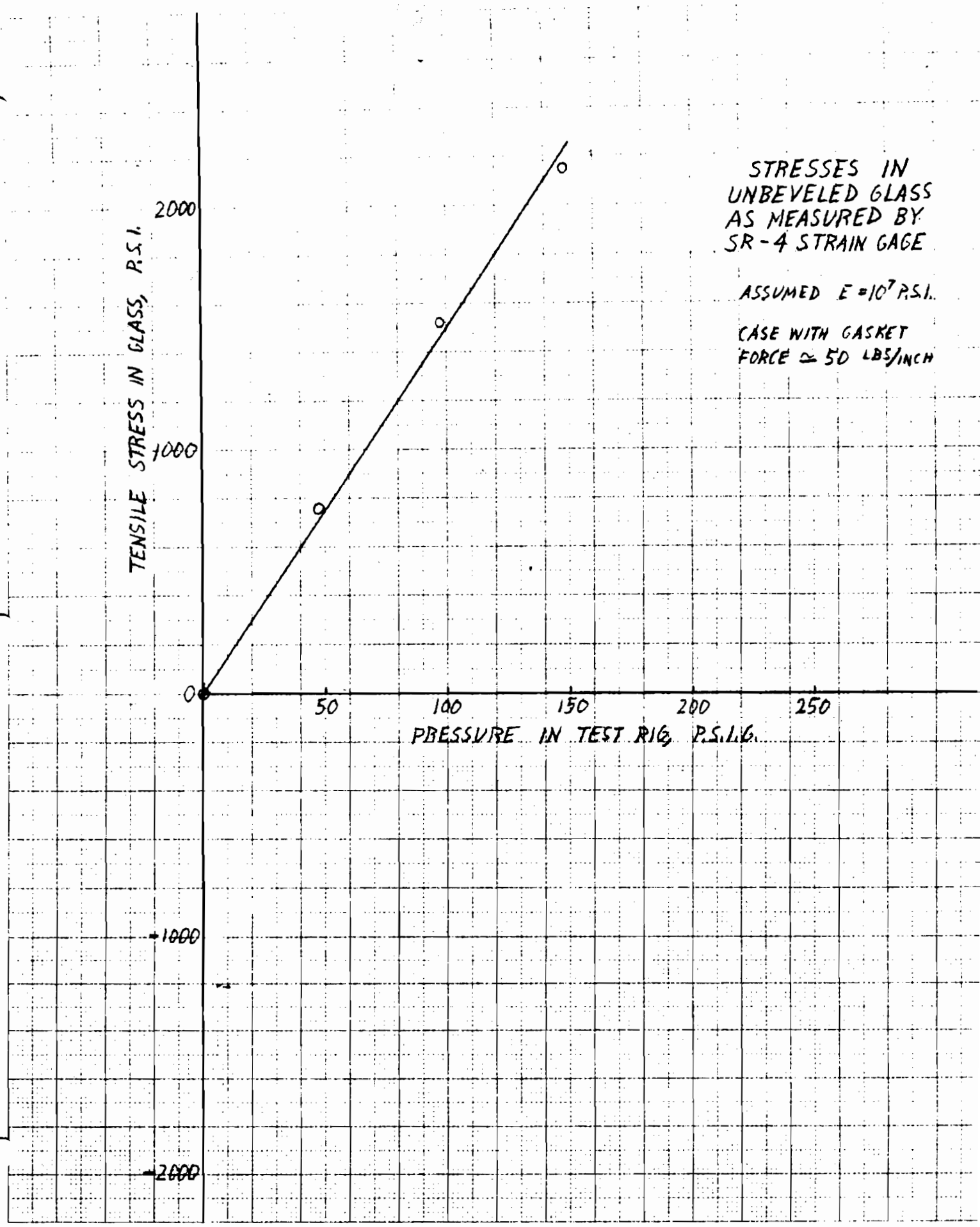
STRESSES IN UNBEVELED GLASS AS MEASURED BY SR-4 STRAIN GAGE
ASSUMED E = 10^7 P.S.I.
CASE WITH GASKET FORCE ≃ 50 LBS/INCH
TENSILE STRESS IN GLASS, P.S.I.
2000
1000
0
-1000
-2000
50
100
150
200
250
PRESSURE IN TEST RIG, P.S.I.G.

FIG. 7

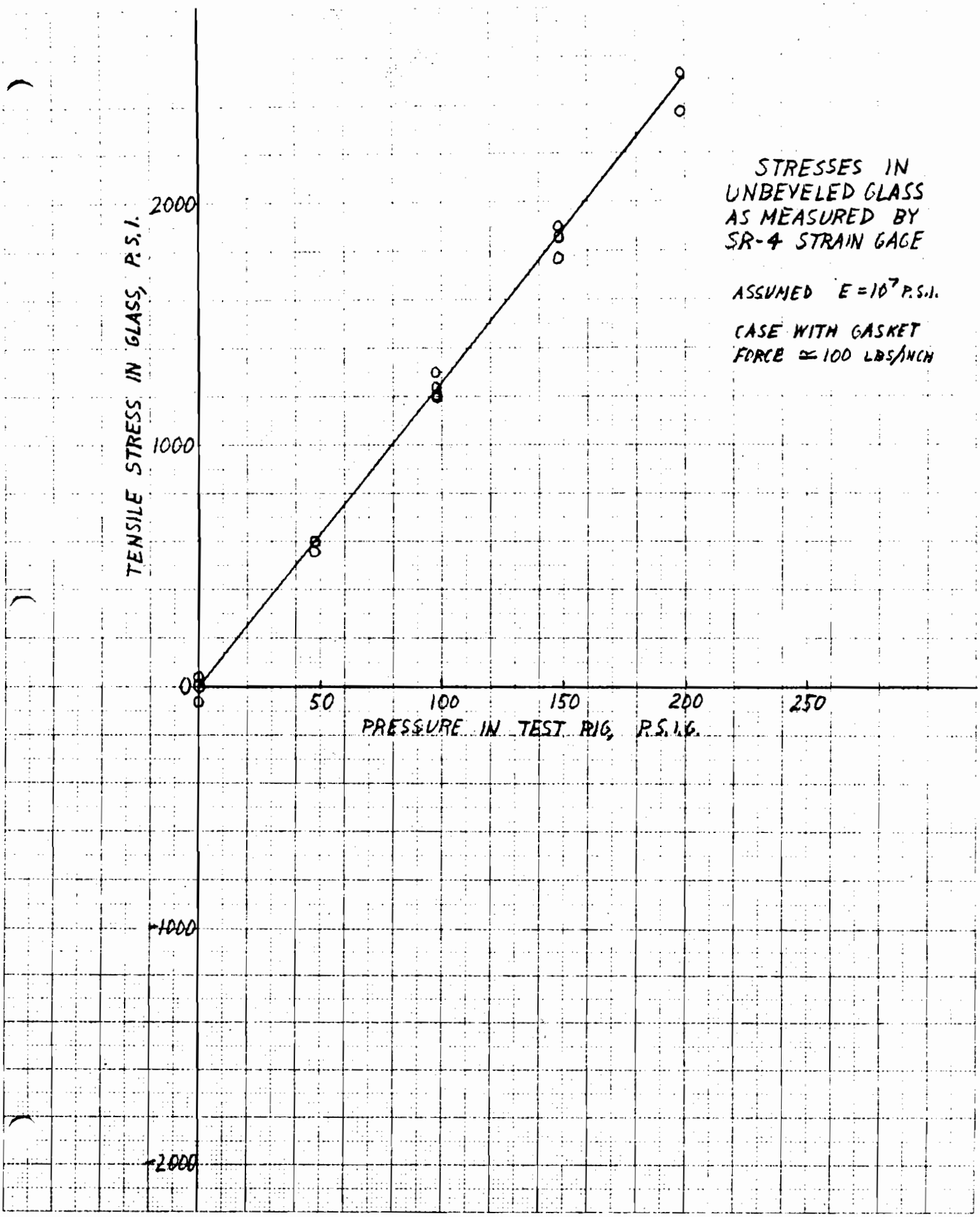
STRESSES IN UNBEVELED GLASS AS MEASURED BY SR-4 STRAIN GAGE
ASSUMED E = 10^7 P.S.I.
CASE WITH GASKET FORCE ≃ 100 LBS/INCH
TENSILE STRESS IN GLASS, P.S.I.
2000
1000
0
-1000
-2000
50
100
150
200
250
PRESSURE IN TEST RIG, P.S.I.G.

FIG. 8

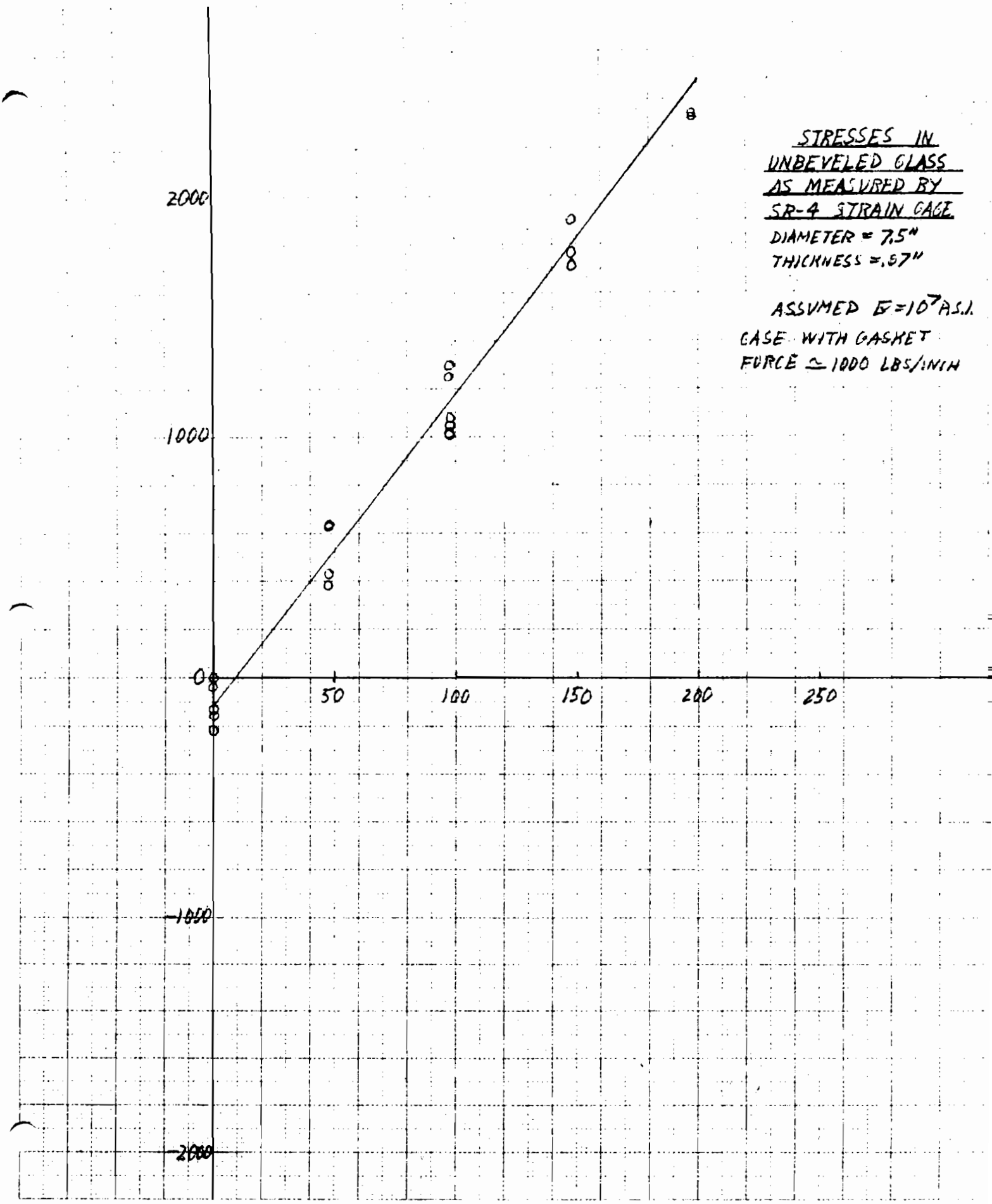
STRESSES IN
UNBEVELED GLASS
AS MEASURED BY
SR-4 STRAIN GAGE
DIAMETER = 7.5"
THICKNESS = .67"
ASSUMED E = 10^7 P.S.I.
CASE WITH GASKET
FORCE ≃ 1000 LBS/INCH
2000
1000
0
-1000
-2000
50
100
150
200
250

FIG. 9

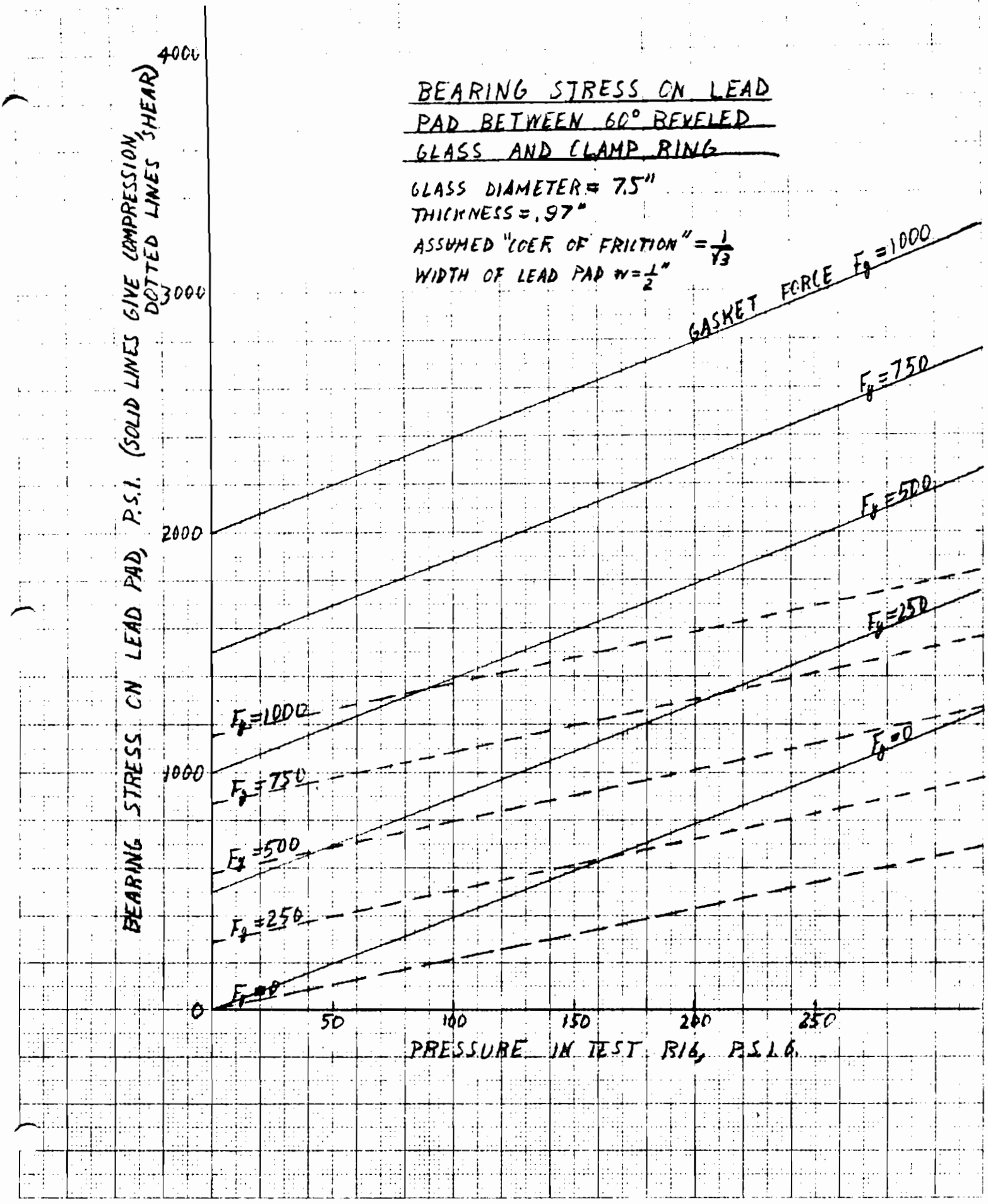
BEARING STRESS ON LEAD PAD BETWEEN 60° BEVELED GLASS AND CLAMP RING
GLASS DIAMETER = 7.5"
THICKNESS = .97"
ASSUMED "COEF OF FRICTION" = 1/√3
WIDTH OF LEAD PAD w = 1/2"
GASKET FORCE Fg = 1000
Fg = 750
Fg = 500
Fg = 250
Fg = 0
Fg = 1000
Fg = 750
Fg = 500
Fg = 250
Fg = 0
BEARING STRESS ON LEAD PAD, P.S.I. (SOLID LINES GIVE COMPRESSION, DOTTED LINES SHEAR)
4000
3000
2000
1000
0
50
100
150
200
250
PRESSURE IN TEST RIG, P.S.I.G.

FIG. 10

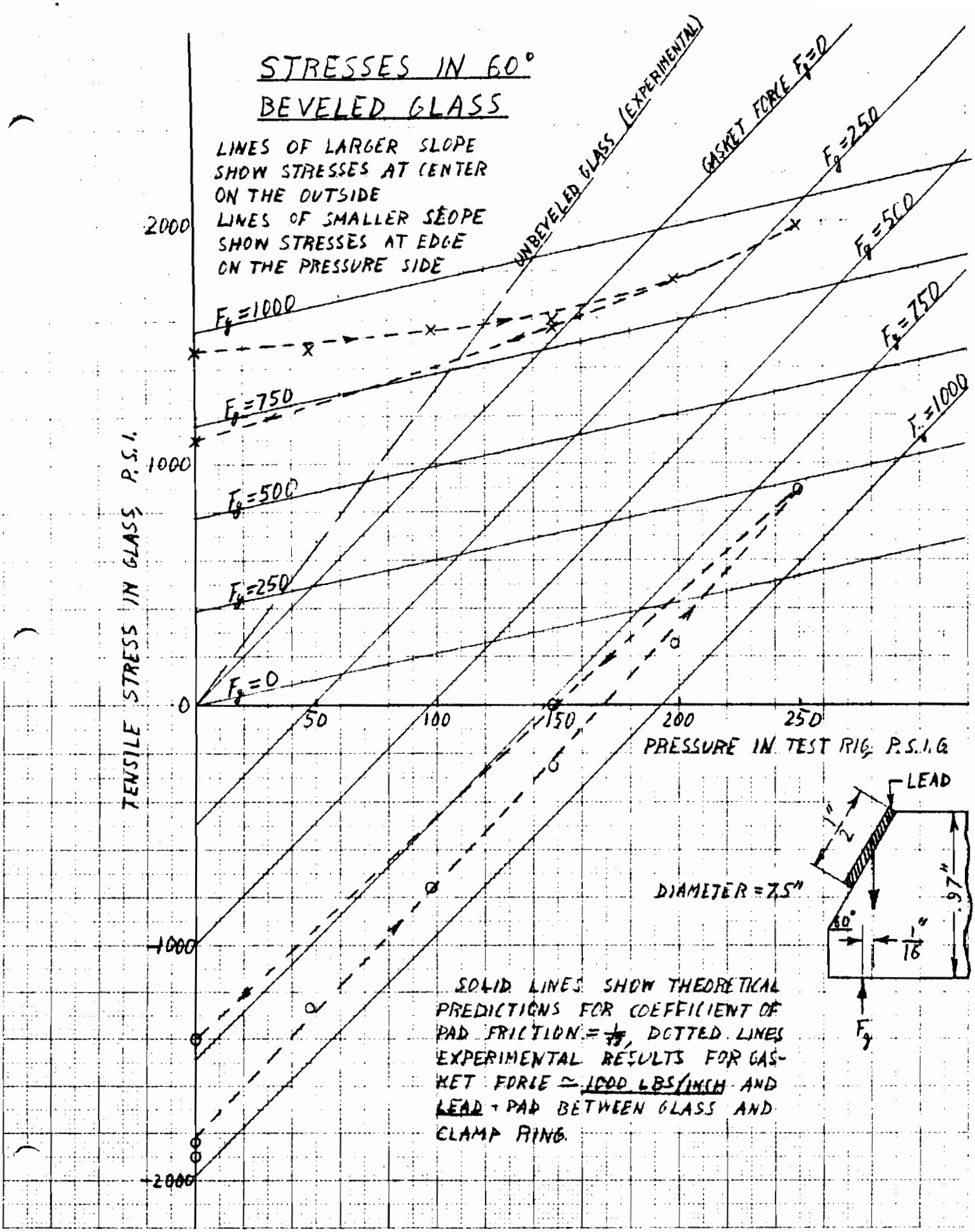
STRESSES IN 60°
BEVELED GLASS
LINES OF LARGER SLOPE
SHOW STRESSES AT CENTER
ON THE OUTSIDE
LINES OF SMALLER SLOPE
SHOW STRESSES AT EDGE
ON THE PRESSURE SIDE
UNBEVELED GLASS (EXPERIMENTAL)
GASKET FORCE F_g=0
F_g=250
F_g=500
F_g=750
F_g=1000
F_g=1000
F_g=750
F_g=500
F_g=250
F_g=0
2000
1000
0
-1000
-2000
50
100
150
200
250
TENSILE STRESS IN GLASS P.S.I.
PRESSURE IN TEST RIG P.S.I.G.
LEAD
1"/2
DIAMETER = 7.5"
.97"
60°
1"/16
F_g
SOLID LINES SHOW THEORETICAL PREDICTIONS FOR COEFFICIENT OF PAD FRICTION = 1/3, DOTTED LINES EXPERIMENTAL RESULTS FOR GASKET FORCE ≃ 1000 LBS/INCH AND LEAD - PAD BETWEEN GLASS AND CLAMP RING.

FIG. 11

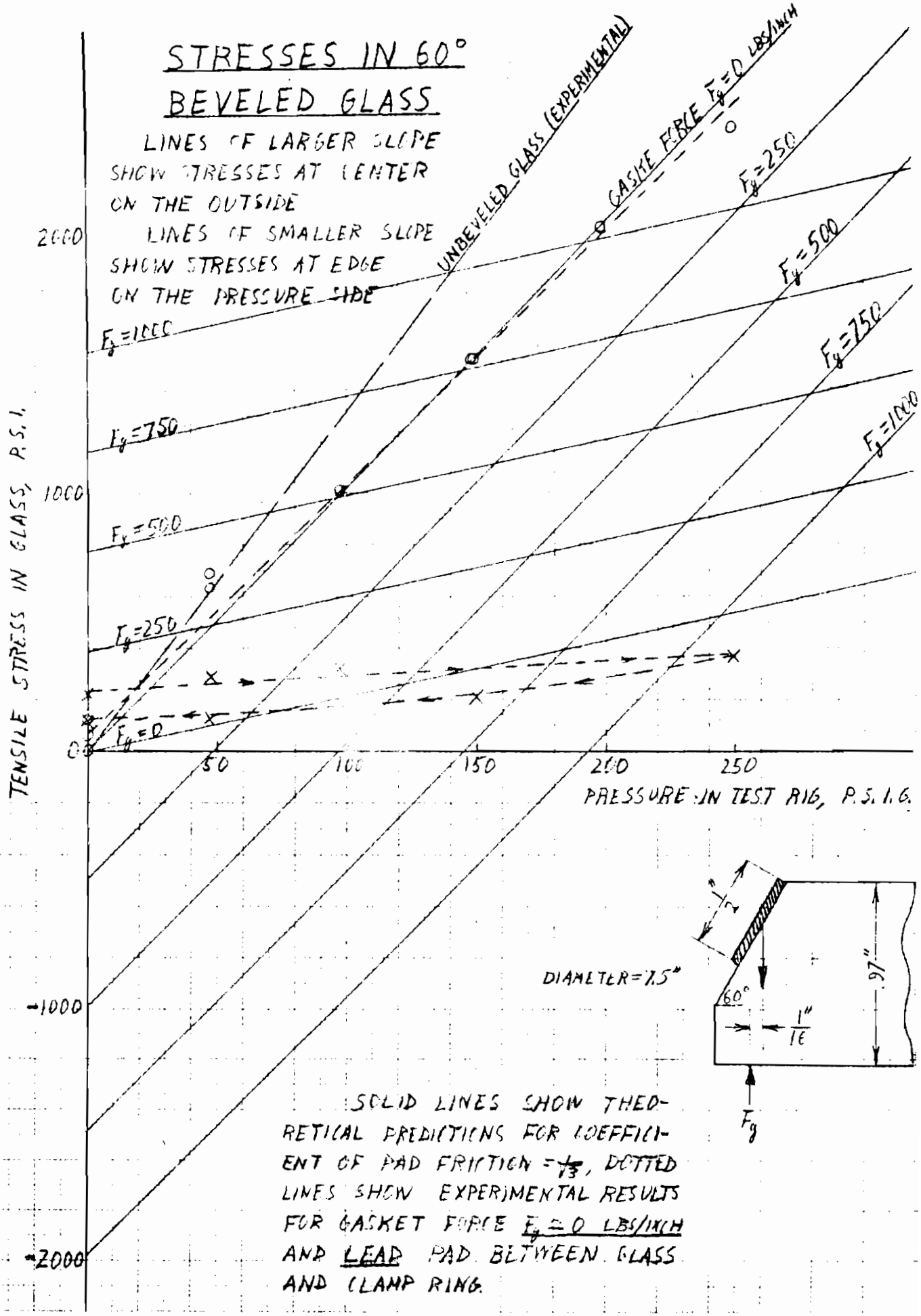
STRESSES IN 60°
BEVELED GLASS
LINES OF LARGER SLOPE SHOW STRESSES AT CENTER ON THE OUTSIDE
LINES OF SMALLER SLOPE SHOW STRESSES AT EDGE ON THE PRESSURE SIDE
UNBEVELED GLASS (EXPERIMENTAL)
GASKET FORCE F_g = 0 LBS/INCH
F_g=250
F_g=500
F_g=750
F_g=1000
F_g=1000
F_g=750
F_g=500
F_g=250
F_g=0
2000
1000
0
-1000
-2000
50
100
150
200
250
TENSILE STRESS IN GLASS, P.S.I.
PRESSURE IN TEST RIG, P.S.I.G.
DIAMETER=7.5"
60°
1"/16
.97"
F_g
SOLID LINES SHOW THEORETICAL PREDICTIONS FOR COEFFICIENT OF PAD FRICTION = 1/3, DOTTED LINES SHOW EXPERIMENTAL RESULTS FOR GASKET FORCE F_g = 0 LBS/INCH AND LEAD PAD BETWEEN GLASS AND CLAMP RING.

FIG. 12

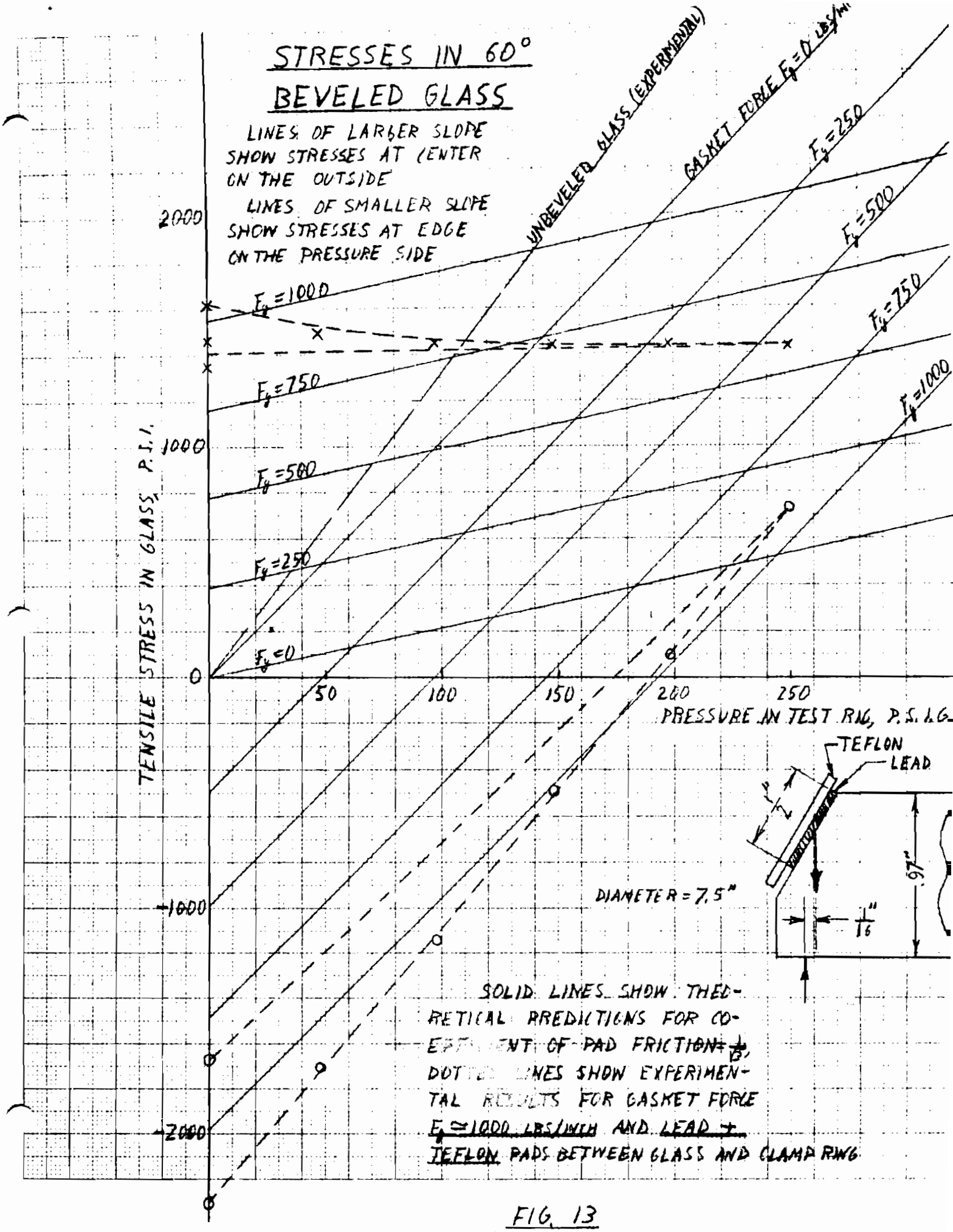
STRESSES IN 60°
BEVELED GLASS
LINES OF LARGER SLOPE SHOW STRESSES AT CENTER ON THE OUTSIDE
LINES OF SMALLER SLOPE SHOW STRESSES AT EDGE ON THE PRESSURE SIDE
UNBEVELED GLASS (EXPERIMENTAL)
GASKET FORCE F_y = 0 LBS/IN.
F_y = 250
F_y = 500
F_y = 750
F_y = 1000
TENSILE STRESS IN GLASS, P.S.I.
2000
1000
0
-1000
-2000
50
100
150
200
250
PRESSURE IN TEST RIG, P.S.I.G.
TEFLON
LEAD
DIAMETER = 7.5"
.97"
1/16"
SOLID LINES SHOW THEORETICAL PREDICTIONS FOR COEFFICIENT OF PAD FRICTION = 1/3, DOTTED LINES SHOW EXPERIMENTAL RESULTS FOR GASKET FORCE F_y ≃ 1000 LBS/INCH AND LEAD + TEFLON PADS BETWEEN GLASS AND CLAMP RING

FIG. 13

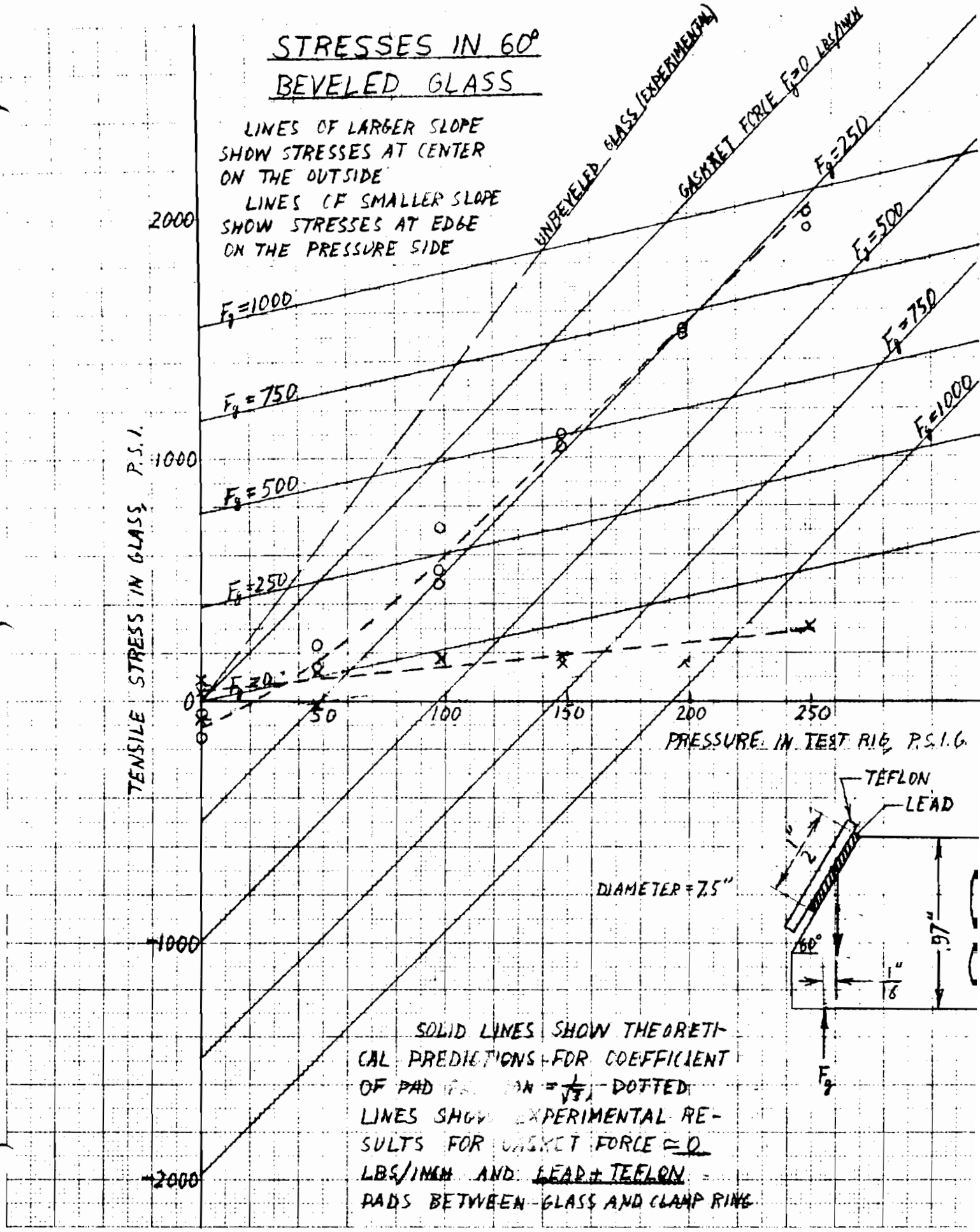
STRESSES IN 60°
BEVELED GLASS
LINES OF LARGER SLOPE SHOW STRESSES AT CENTER ON THE OUTSIDE
LINES OF SMALLER SLOPE SHOW STRESSES AT EDGE ON THE PRESSURE SIDE
UNBEVELED GLASS (EXPERIMENTAL)
GASKET FORCE F_g=0 LBS/INCH
F_g=250
F_g=500
F_g=750
F_g=1000
F_g=1000
F_g=750
F_g=500
F_g=250
F_g=0
2000
1000
0
-1000
-2000
50
100
150
200
250
TENSILE STRESS IN GLASS P.S.I.
PRESSURE IN TEST RIG P.S.I.G.
TEFLON
LEAD
DIAMETER = 7.5"
60°
.97"
1/16"
F_g
SOLID LINES SHOW THEORETICAL PREDICTIONS FOR COEFFICIENT OF PAD FRICTION = $\frac{1}{\sqrt{3}}$, DOTTED LINES SHOW EXPERIMENTAL RESULTS FOR GASKET FORCE ≃ 0 LBS/INCH AND LEAD + TEFLON PADS BETWEEN GLASS AND CLAMP RING

FIG. 14

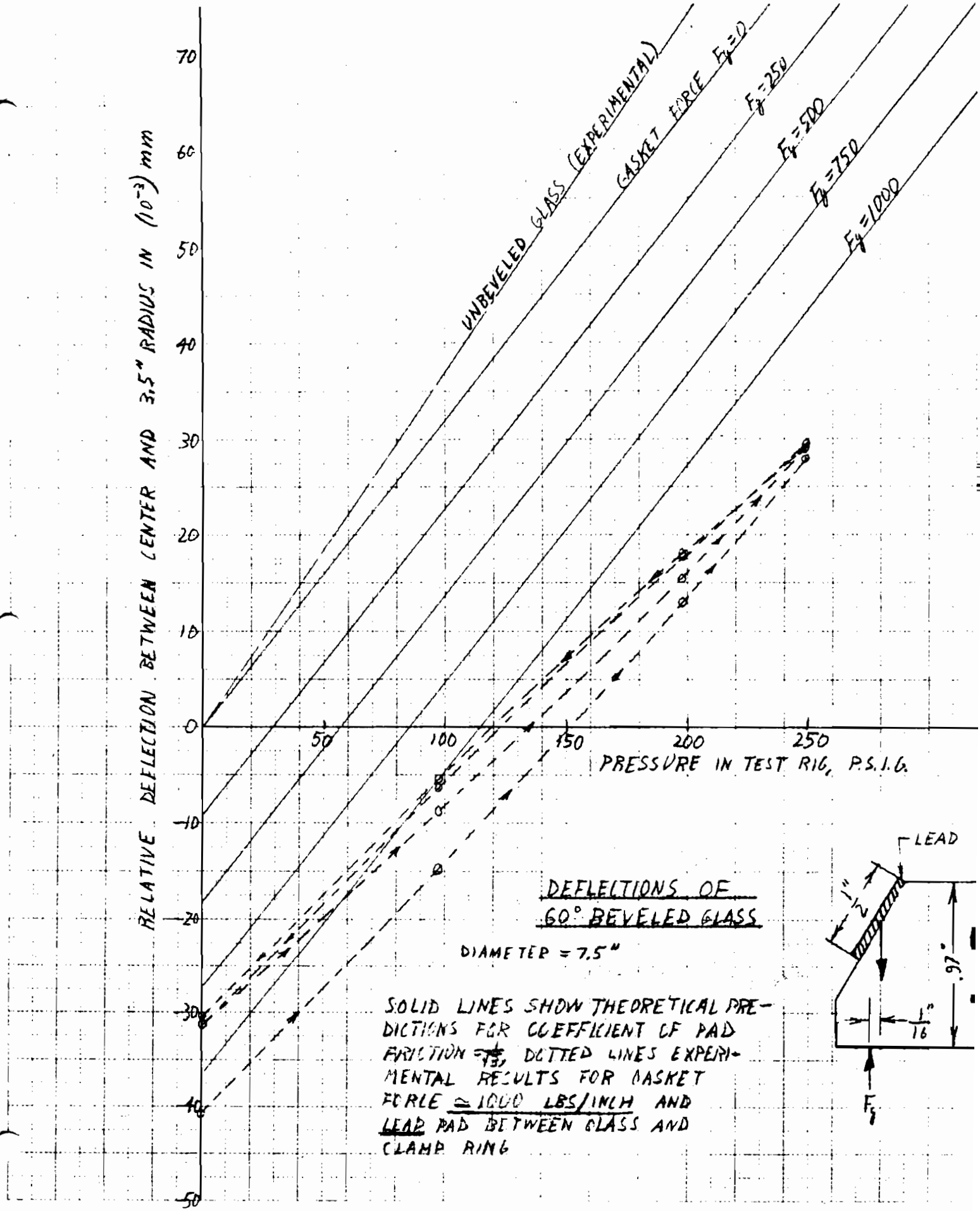
RELATIVE DEFLECTION BETWEEN CENTER AND 3.5" RADIUS IN (10^{-3}) mm
70
60
50
40
30
20
10
0
-10
-20
-30
-40
-50
50
100
150
200
250
PRESSURE IN TEST RIG, P.S.I.G.
UNBEVELED GLASS (EXPERIMENTAL)
GASKET FORCE $F_g = 0$
$F_g = 250$
$F_g = 500$
$F_g = 750$
$F_g = 1000$
DEFLECTIONS OF 60° BEVELED GLASS
DIAMETER = 7.5"
SOLID LINES SHOW THEORETICAL PREDICTIONS FOR COEFFICIENT OF PAD FRICTION = .15, DOTTED LINES EXPERIMENTAL RESULTS FOR GASKET FORCE ≃ 1000 LBS/INCH AND LEAD PAD BETWEEN GLASS AND CLAMP RING
LEAD
1/2"
.97"
1/16"
F_g

FIG. 15

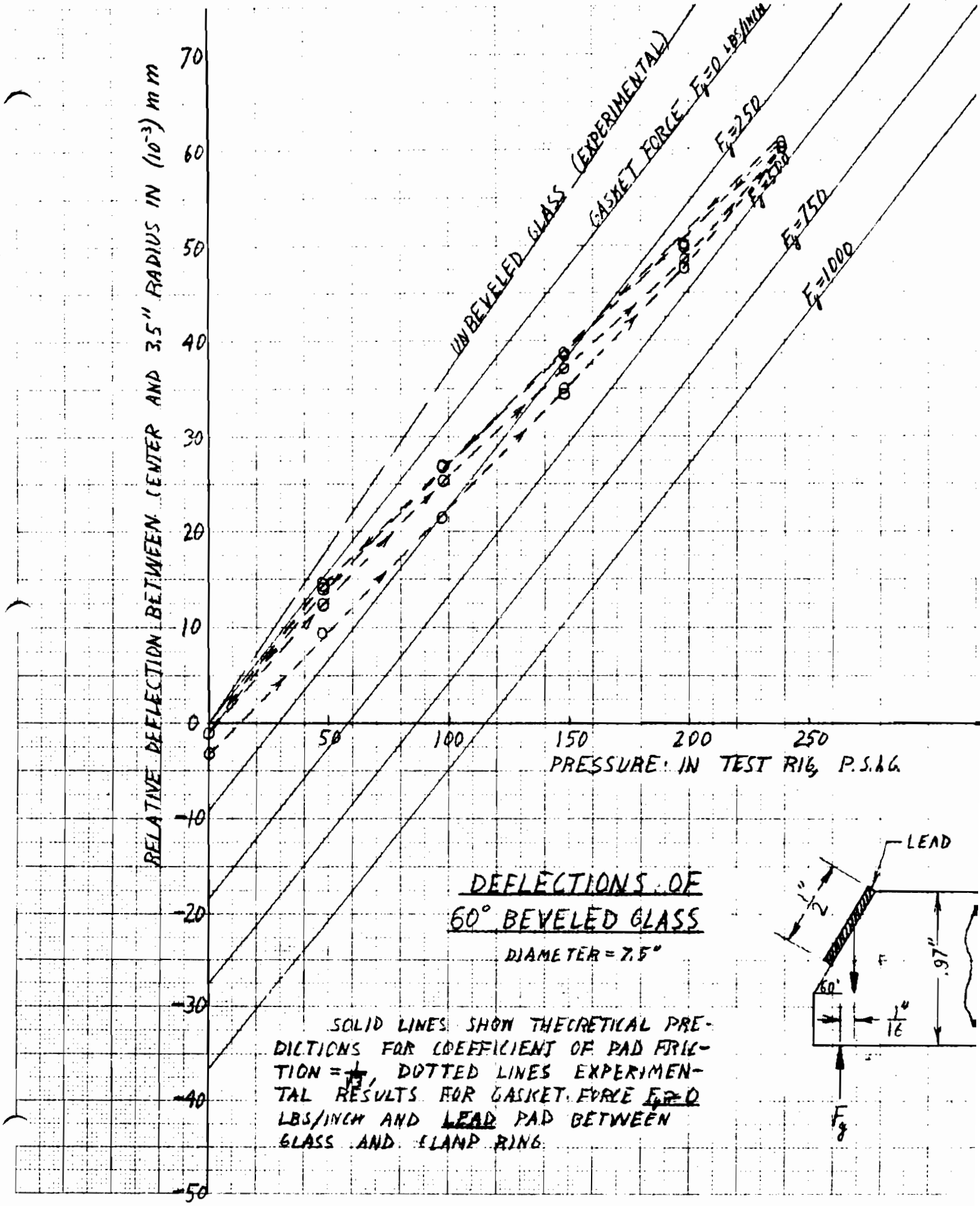
RELATIVE DEFLECTION BETWEEN CENTER AND 3.5" RADIUS IN (10^{-3}) mm
70
60
50
40
30
20
10
0
-10
-20
-30
-40
-50
50
100
150
200
250
PRESSURE IN TEST RIG, P.S.I.G.
UNBEVELED GLASS (EXPERIMENTAL)
GASKET FORCE F_g=0 LBS/INCH
F_g=250
F_g=500
F_g=750
F_g=1000
DEFLECTIONS OF
60° BEVELED GLASS
DIAMETER = 7.5"
SOLID LINES SHOW THEORETICAL PREDICTIONS FOR COEFFICIENT OF PAD FRICTION = $\frac{1}{\sqrt{3}}$, DOTTED LINES EXPERIMENTAL RESULTS FOR GASKET FORCE F_g=0 LBS/INCH AND LEAD PAD BETWEEN GLASS AND CLAMP RING
LEAD
1/2"
.97"
60°
1/16"
F_g

FIG. 16

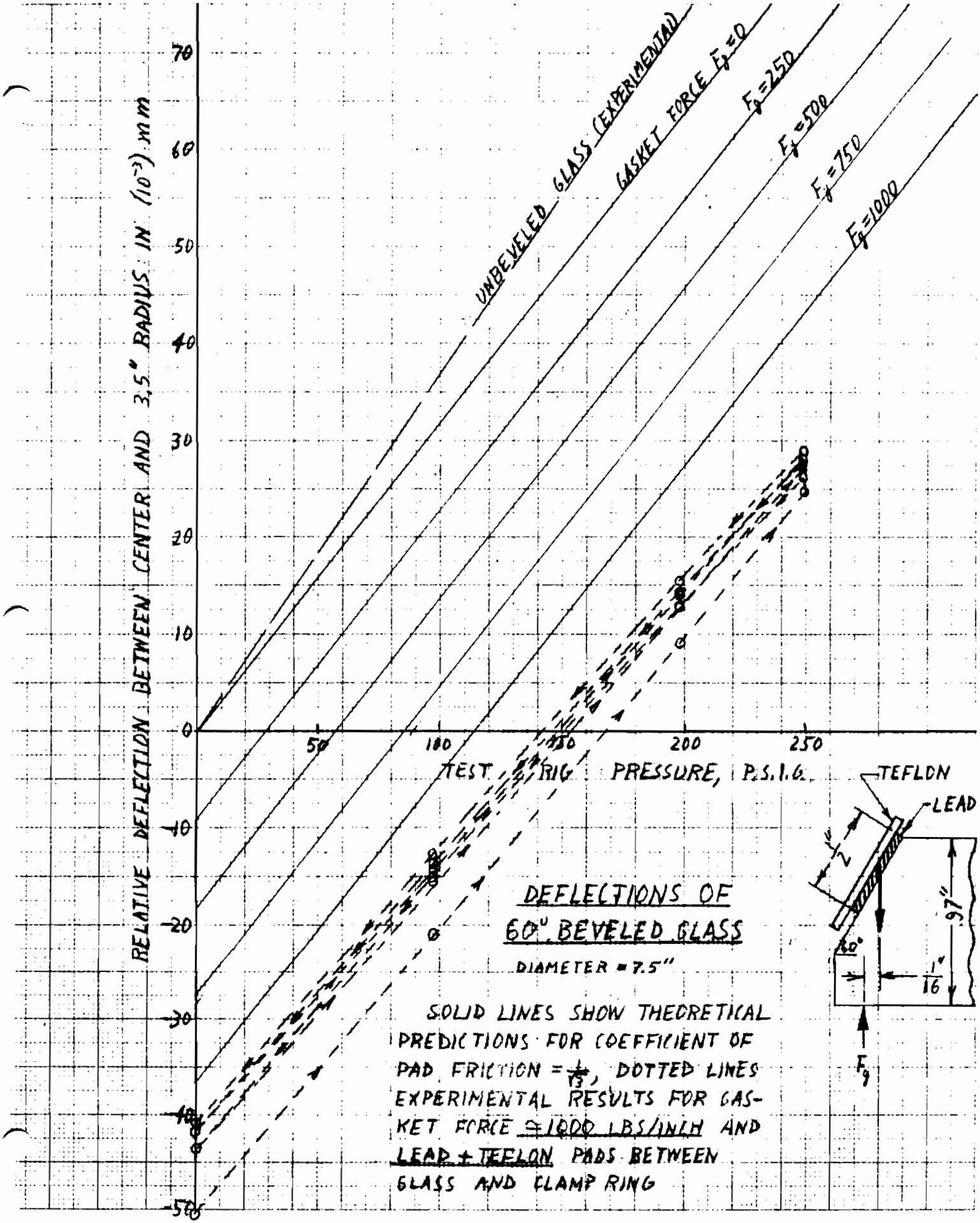
RELATIVE DEFLECTION BETWEEN CENTER AND 3.5" RADIUS IN (10^{-3}) mm
70
60
50
40
30
20
10
0
-10
-20
-30
-40
-50
50
100
150
200
250
TEST RIG PRESSURE, P.S.I.G.
UNBEVELED GLASS (EXPERIMENTAL)
GASKET FORCE $F_g = 0$
$F_g = 250$
$F_g = 500$
$F_g = 750$
$F_g = 1000$
DEFLECTIONS OF
60° BEVELED GLASS
DIAMETER = 7.5"
SOLID LINES SHOW THEORETICAL PREDICTIONS FOR COEFFICIENT OF PAD FRICTION = $\frac{1}{\sqrt{3}}$, DOTTED LINES EXPERIMENTAL RESULTS FOR GASKET FORCE ≈ 1000 LBS/INCH AND LEAD + TEFLON PADS BETWEEN GLASS AND CLAMP RING
TEFLON
LEAD
2"
.97"
60°
1/16"
F_g

FIG. 17

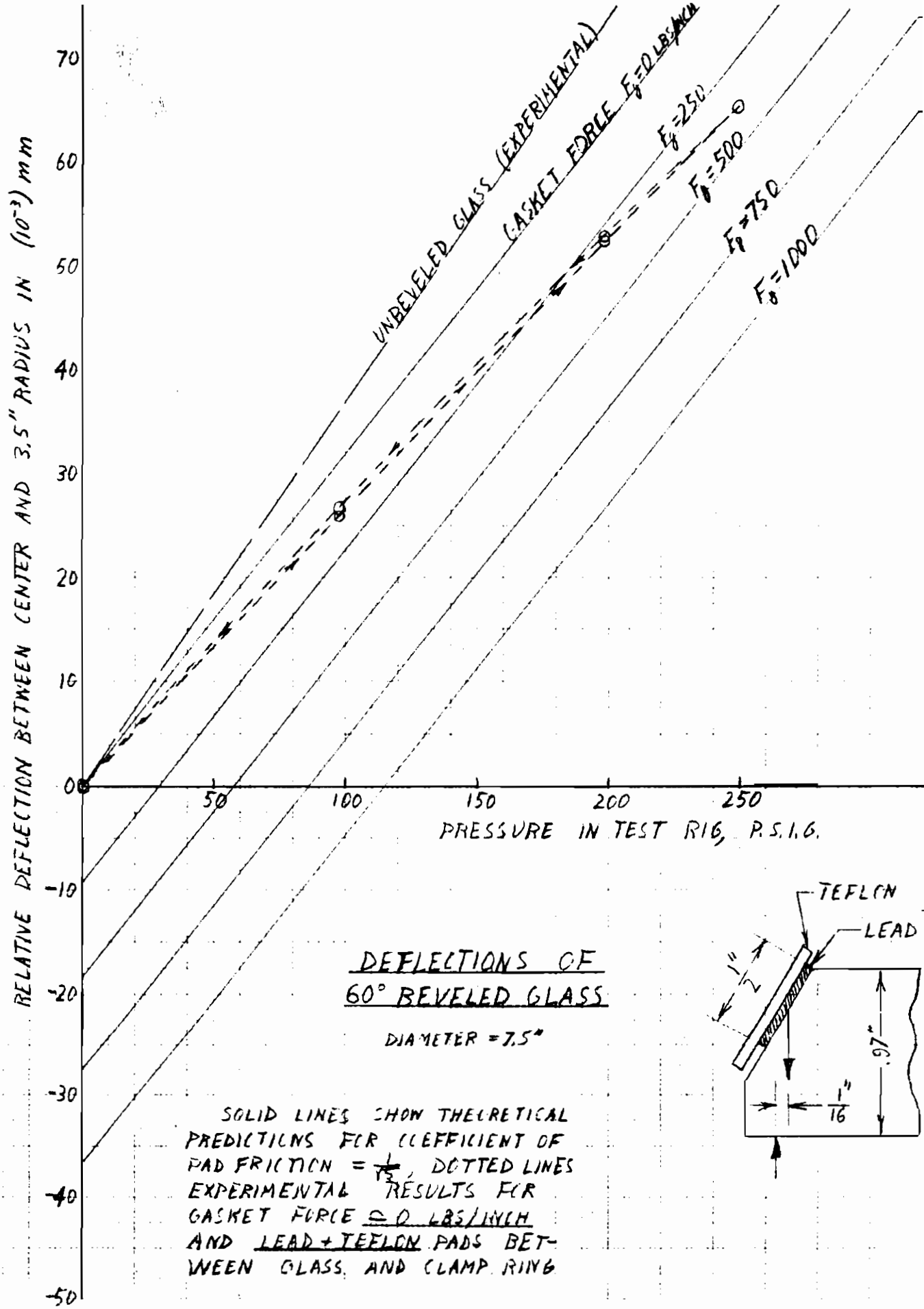
UNBEVELED GLASS (EXPERIMENTAL)
(GASKET FORCE F_g=0 LBS/INCH)
F_g=250
F_g=500
F_g=750
F_g=1000
RELATIVE DEFLECTION BETWEEN CENTER AND 3.5" RADIUS IN (10^{-3}) mm
70
60
50
40
30
20
10
0
-10
-20
-30
-40
-50
50
100
150
200
250
PRESSURE IN TEST RIG, P.S.I.G.
TEFLON
LEAD
1/2"
.97"
1/16"
DEFLECTIONS OF
60° BEVELED GLASS
DIAMETER = 7.5"
SOLID LINES SHOW THEORETICAL PREDICTIONS FOR COEFFICIENT OF PAD FRICTION = 1/√3, DOTTED LINES EXPERIMENTAL RESULTS FOR GASKET FORCE ≅ 0 LBS/INCH AND LEAD + TEFLON PADS BETWEEN GLASS AND CLAMP RING

FIG. 18

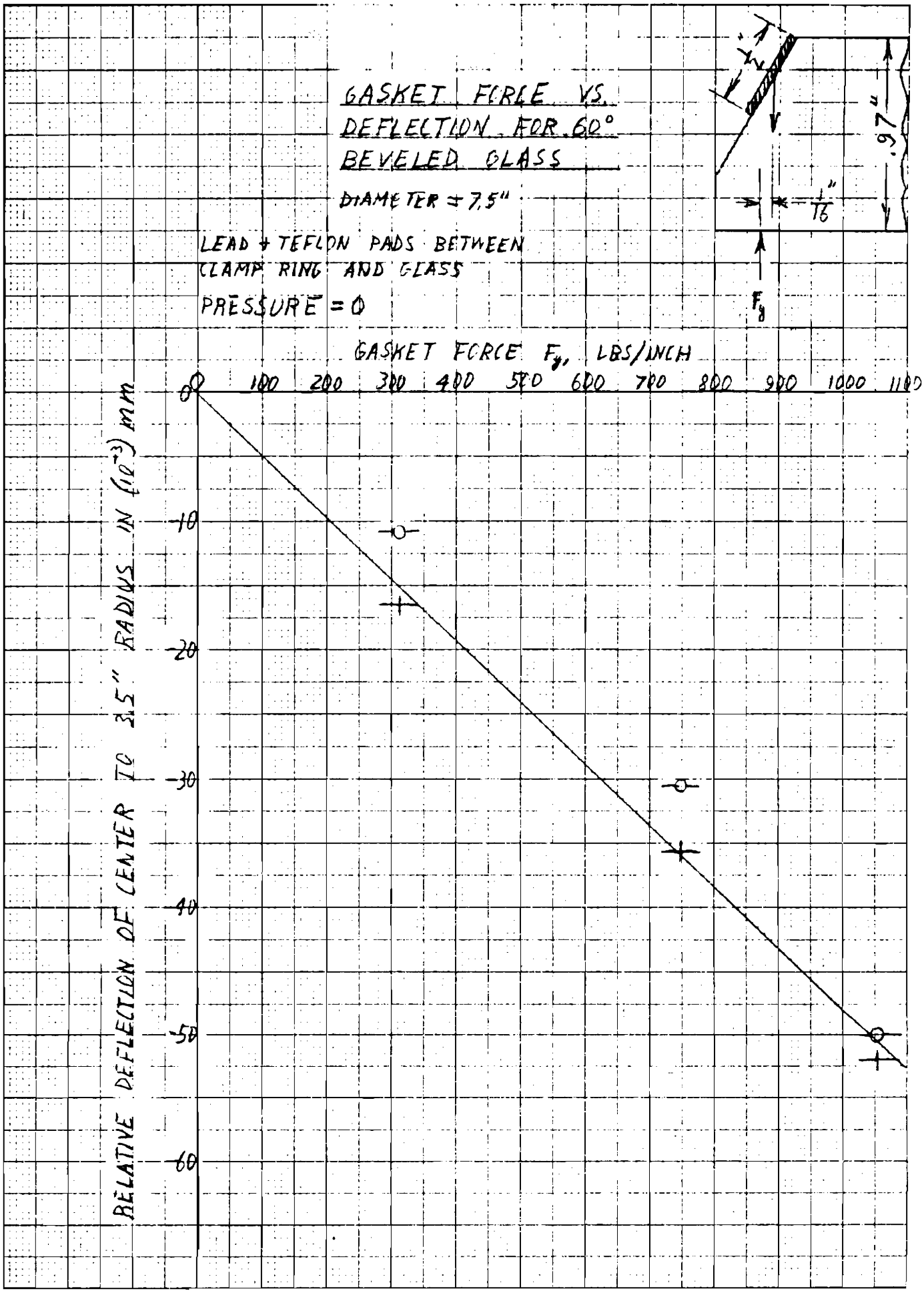

FIG. 19

ULRICH'S BOOK STORE ANN ARBOR, MICH.
10 X 10 TO THE 1/2 INCH 359-11 KEUFFEL & ESSER CO.

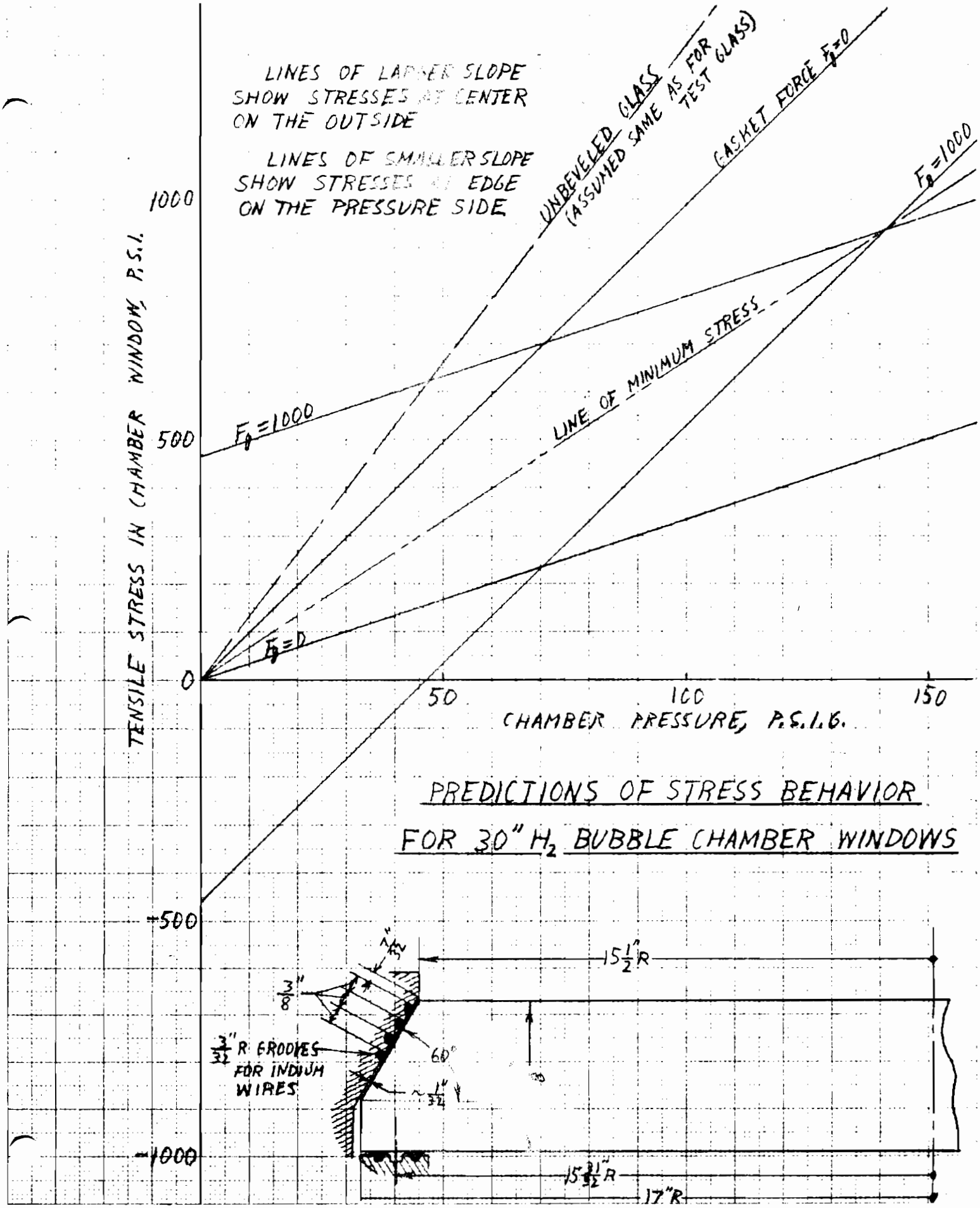

PREDICTIONS OF STRESS BEHAVIOR FOR 30" H_2 BUBBLE CHAMBER WINDOWS

FIG. 20

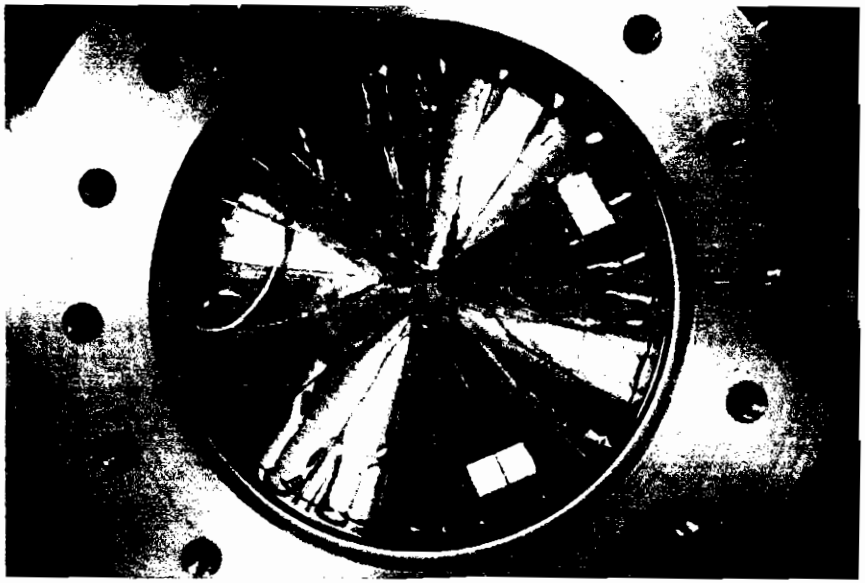

Figure 21: Beveled glass, with mounting pad width = 1/2", leaking after cracking at 700 psi pressure, then taken to 1000 psi and lowered to zero pressure.

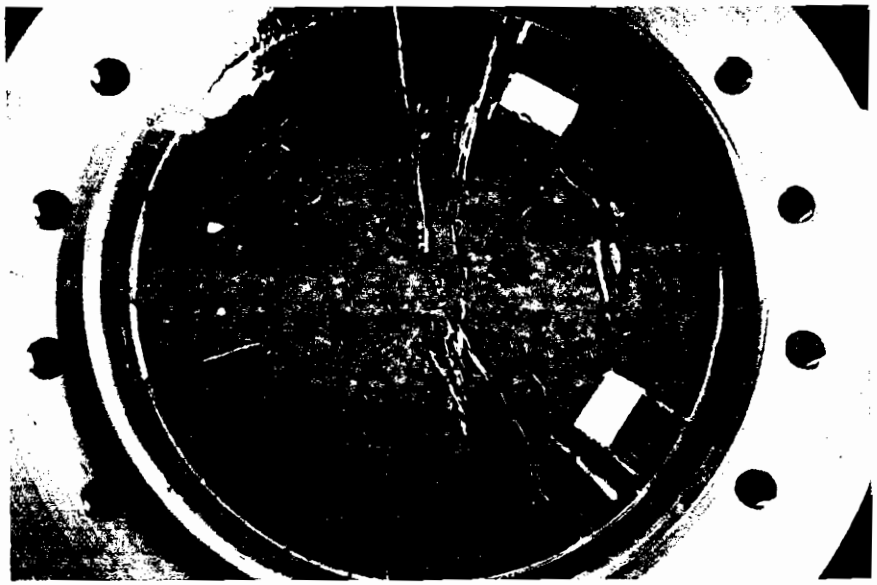

Figure 22: Underside of the same glass as in Figure 21, after disassembly of test fixture.

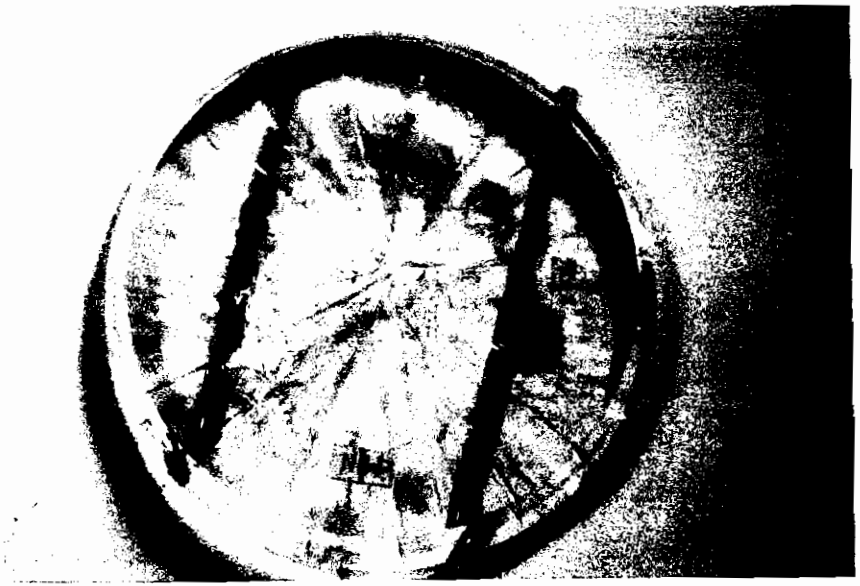

Figure 23: Same piece of glass again; here we can see how it hung together after being lifted out.

Figure 24: Same glass; here seen after it fell apart upon further handling.

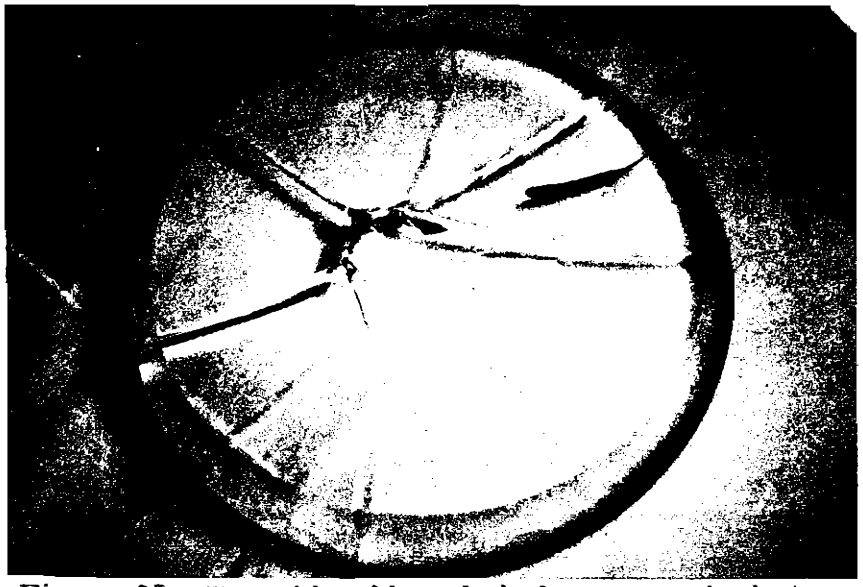

Figure 25: Top side of beveled glass, cracked at 300 psi pressure with mounting pad width = 3/8".

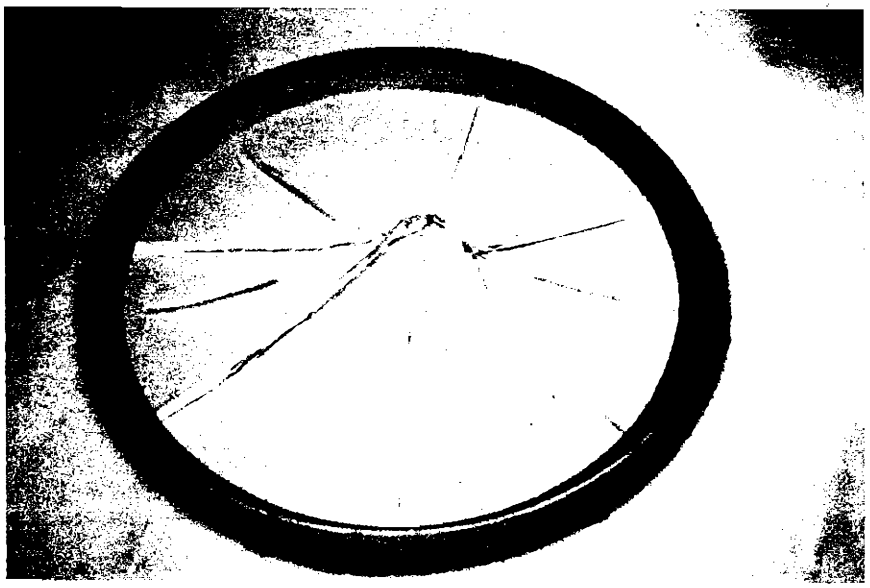

Figure 26: Bottom side of same glass as in Figure 25. Here it can be seen that no crack goes all the way through.

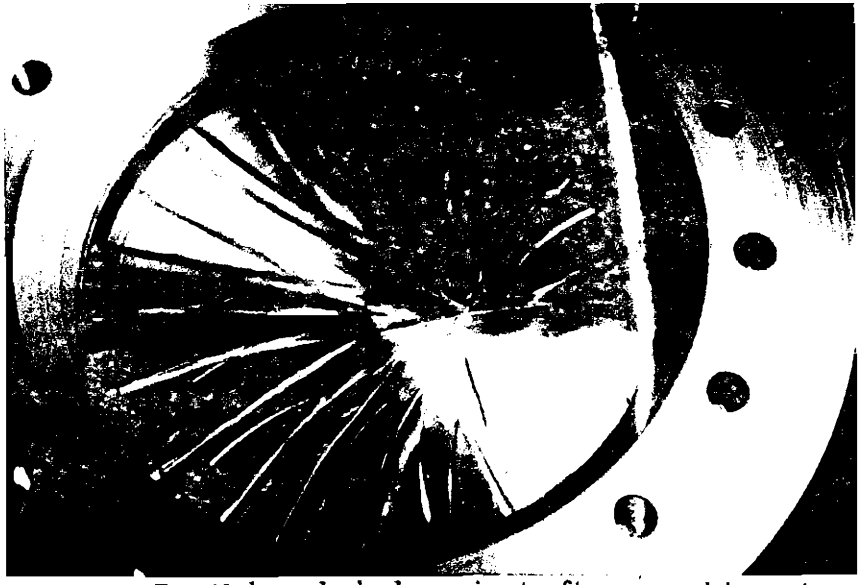

Figure 27: Unbeveled glass just after cracking at 300 psi pressure.

Figure 28: Same glass as in Figure 27; fell apart as test fixture was disassembled.